PEOPLE'S DEMOCRATIC REPUBLIC OF ALGERIA
MINISTRY OF HIGHER EDUCATION AND SCIENTIFIC RESEARCH
MOHAMED BOUDIAF UNIVERSITY - M'SILA

FACULTY OF: TECHNOLOGY

DEPARTMENT OF: ELECTRONICS

N°:

FIELD OF STUDY: ELECTRONICS

SPECIALIZATION: MICROELECTRONICS

Thesis presented for the attainment

of the Academic Master's degree

by: ZEROUAK NESSRINE

MAHMOUDI IMANE

THEME

Hybrid Parameters Extraction Procedure of PV Module in Real Working Condition

Defended before the jury composed of:

Pr. MEZAACHE AMMAR	*Mohamed Boudiaf University of M'Sila*	President
Pr. OUDIRA HOUCINE	*Mohamed Boudiaf University of M'Sila*	Supervisor
Dr. KAHLOUCHE AHMED	*Mohamed Boudiaf University of M'Sila*	Examinator

Academic year:2023/ 2024

Abstract:

The identification of photovoltaic (PV) model parameters under real operating conditions is a crucial step for energy forecasting. An accurate and reliable model depends mainly on the precision of its parameters. In this work, a precise methodology is developed for extracting PV module parameters under real conditions. The proposed methodology combines numerical methods and analytical formulations of the diode model to derive the five unknown parameters under any operating condition of irradiance and temperature. First, measured (I-V) curves under random weather conditions are transformed into standard test conditions (i.e., G = 1000 W/m², T = 25 °C) using translation equations. The second step involves using an optimization algorithm to identify the five parameters under standard conditions. Analytical formulations, under random irradiance and temperature, are then used to express the unknown parameters under any irradiance and temperature. The proposed approach will be validated under outdoor conditions compared to measured I-V curves under different operating conditions. Dynamic validation is also performed where the measured values of the maximum power point (MPP) coordinates are compared to the actual dynamic MPP measurements of a grid-connected system located at the Renewable Energy Development Center (CDER) in Algiers.

Keywords: Extraction, optimization, real conditions, dynamic validation

Résumé:

L'identification des paramètres du modèle photovoltaïque (PV) dans des conditions d'exploitation réelles est une étape cruciale pour la prévision énergétique. Un modèle précis et fiable dépend principalement de la précision des paramètres du modèle. Dans ce travail, une méthodologie précise est destinée pour l'extraction des paramètres du module PV dans des conditions réelles. La méthodologie proposée combine des méthodes numériques et des formulations analytiques du modèle à une diode pour dériver les cinq paramètres inconnus dans n'importe quelle condition de fonctionnement d'irradiance et de température. Tout d'abord, les courbes (I-V) mesurées dans des conditions météorologiques aléatoires sont transformées en conditions de test standard (c'est-à-dire, G = 1000 W/m2, T = 25 °C), en utilisant des équations de translation. La deuxième étape consiste à utiliser un algorithme d’optimisation pour identifier

les cinq paramètres dans des conditions standard. Des formulations analytiques, à éclairement et température aléatoires, sont ensuite utilisées pour exprimer les paramètres inconnus à n'importe quelle éclairement et température. L'approche proposée sera validée dans des conditions extérieures par rapport aux courbes I-V mesurées dans différentes conditions de fonctionnement. La validation dynamique est également effectuée où la valeur mesurée des coordonnées du point de puissance maximale (MPP) sont comparées aux mesures dynamiques réelles MPP d'un système connecté au réseau situé dans le Centre de Développement des Energies Renouvelables (CDER) à Alger.

Mots clés : Extraction, optimisation, conditions réelles, validation dynamique

ملخص:

تحديد معلمات نموذج الطاقة الشمسية (PV) في ظروف التشغيل الحقيقية خطوة حاسمة للتنبؤ بالطاقة. يعتمد نموذج دقيق و موثوق في المقام الأول على دقة معاملماته .في هذا العمل ,تم تطوير منهجية دقيقة لاستخراج معلمات وحدة PV في ظروف حقيقية. تجمع المنهجية المقترحة بين الأساليب العددية و التركيبات التحليلية في نموذج الصمام (Diode) لاستنباط الخمس معلمات المجهولة تحت أي شرط تشغيل للإشعاع الشمسي و درجة الحرارة. في الخطوة الأولى، تتم تحويل النقاط المقاسة (I-V) في ظروف جوية عشوائية إلى شروط اختبار قياسية (أي $G=1000\ W/m^2$، $T=25°$ باستخدام معادلات الترجمة. الخطوة الثانية تنطوي على استخدام خوارزمية الأمثلية لتحديد الخمسة معلمات تحت الشروط القياسية. يتم استخدام التركيبات التحليلية، تحت الإشعاع و درجة الحرارة العشوائية، بعد ذلك للتعبير عن المعلمات المجهولة تحت أي إشعاع و درجة حرارة. سيتم تحقيق النهج المقترح في ظروف الهواء الطلق مقارنة بالنقاط المقاسة (I-V) تحت ظروف تشغيل مختلفة. كما يتم تنفيذ التحقق الديناميكي حيث يتم مقارنة القيم المقاسة لنقاط القدرة القصوى (MPP) بالقياسات الديناميكية الفعلية MPP لنظام متصل بالشبكة يقع في مركز تطوير الطاقة المتجددة (CDER) في الجزائر.

الكلمات الرئيسية: استخراج، أمثلية، ظروف حقيقية، التحقق الديناميكي.

Acknowledgments

I would like to express my gratitude to all the individuals and institutions who contributed, directly or indirectly, to the completion of this thesis.

First and foremost, I would like warmly to thank my thesis supervisor, ***Pr. Houcine Oudira****, for his valuable advice, unwavering support, and insightful comments throughout this project. His encouragement and his trust have been essential drivers in completing this research.*

I would like to thank ***Pr. Mezache Amar*** *for being president of the examination committee. I also would like to thank my oral thesis committee member* ***Dr. Kahlouche Ahmed*** *for accepting the examination of this thesis.*

I also wish to thank the faculty members of the Electronic at University Mouhamed Boudiaf M'silafor their quality teaching and guidance, which allowed me to deepen my knowledge and develop the necessary skills for preparing this thesis.

I am also grateful to my fellow students for their support, camaraderie, and constructive exchanges that enriched this experience. The stimulating discussions and moments of solidarity greatly contributed to making this academic journey more enjoyable.

Finally, I thank all the people who, directly or indirectly, contributed to the completion of this thesis, especially the participants in my study, without them this work would not have been perfect.

إهـداء

بسم الله الرحمان الرحيم

الحمد والشكر لله وحده على توفيقه وكرمه .

لكل شيىء نهاية وهاهي اجمل نهايات حياتي تكتب على شكل اهداء اعود ايه كلما اشتقت لأيام مرت ولن تتكرر .

هي أيام مرت بحلوها ومرها وتركت في قلبي ذكريات مميزة واشخاص كانوا السند .

الى قرة عيني الذي جعل هذا الاهداء يستغرق ليلة كاملة لإتمامه الذي اعجز عن وصفه الي أبي وحبيبي محمد زرواق الذي لطالما كان نقطة البداية والنهاية والضعف الي روح الروح الذي ساندني ولم يكل ولم يمل يوما انار الله حياتك يانور حياتي .

الي سعادتي ومهربي وأماني توأم روحي الي أمي الحبيبة زهية الي التي تعيد لي الروح في اضعف ايامي كنت لي الركن اللين الهين الذي ينشر البهجة حتى وإن مرعلى البال جعل الله ايامكي بهجة وسرورا حبيبتي.

الي ظلعي الثابت مهما هزتني الأيام الي التي بفظلها اكتب هذه الاسطر اليوم الي اميرتي اختي حبيبتي دمتي اميرة جميلة تزهر ايامي .

الي سندي ومسندي الي حبيب اخته الوحيد حظي في هذه الحياة الى مترجمي الماهر أسامة زرواق .

الي صغيرة البيت ونوره الي ابنتي العبقرية نور جعلكي الله فخر العائلة

الي كل عائلتي بدون استثناء عمو عبد الحكيم خالتي نورة.... ملك .... اسيل .....اسلام ..

الى جدتي خيرة وزينب .

الى الذين غابوا عن الدنيا ولم يغيبواعن قلبي جدي مفتاح ومحاد خالي الذوادي وخالتي زهوة رحمهم الله.

الي صديقاتي وزملائي الذين عشت معهم اسعد ايامي ... ايمان محمودي ... عبير ميشالي ... هاجر جناوي.

الى اساتذتي الافاضل حسين اوديرا ... دربال عميروش ... عبيدة شرحبيل ..

الى كل من علمني حرفا وساندني بموقف اهديكم ثمرة نجاحي

الحمد والشكر لله تعالى .

نسرين زرواق

إهـداء

إلهي لاتطيب اللحظات إلى بشكرك وحمدك .فاللهم لك الحمد والشكر .لأنك وفقتني على إنهاء هذا العمل وتحقيق حلمي .

ماسلكنا البدايات الا بتسيره ومابلغنا النهايات الل بتوفيقه وماحققنا الغايات إلى بفضله فالحمد لله الذي وفقنا لتثمين هذه الخطوة .

اهدي نجاحي هذا :

إلى من قال فيهما الله تعالى :"وقضى ربك الا تعبدو الا اياه وبالوالدين احسانا".

إلى من كلل العرق جبينه ومن علمني ان النجاح لايأتي الا بالصبر والإصرار إلى النور الذي أنار دربي والسراج الذي لا ينطفئ نوره بقلبي ابدا من بذل الغالي والنفيس واستمديت منه قوتي واعتزازي بذاتي إلى ابي الغالي .

إلى من جعل الجنة تحت اقدامها وسهلت لي الشدائد بدعائها إلى امي الغالية.

إلى ظلعي الثابت وامان ايامي إلى من شددت عضدي بهم فكانوا انابيع ارتوي منها إلى خيرة ايامي وصفوتها إلى قرة عيني إلى اخي كريم واخواتي رزيقة ،بشرى .

إلى من هو جزء من الروح إلى حبيبي ابن أختي سند ايهاب ،وإلى فلذت كبدي برعمي جواد .

إلى الذين ذهبوا وحملهم قلبي بالدعاء ومشاعري بالفقد والحزن ها أنا اشاركهم نجاحي إلى فيقيدي : إلى خالي عبد الله رحمه الله وإلى صديقتي فاطمة الزهراء رحمها الله .

لكل من كان عونا وسند في هذا الطريق لصديقاتي وفياء رفقات السنين لصاحبات الشدائد والازمات :نسرين ،هاجر،عبير ،بثينة،دنيازاد ،خولة،مريم ،امال.

إلى من هم قطعة من روح إلى بنات خلاتي :احلام ،أمينة .

إلى من كان له الفضل في إنجاز بحثي هذا الى الذي لم يبخل عليا بشيء أستاذي الفاضل :حسين اوديرا .

إلى من أفاضني بمشاعره ونصائحه وإليكم كافة عائلتي اهديكم انجازي وثمرة نجاحي لطالما تمنيته أنا اليوم أكملت واتممت أول ثمراته بفضله سبحانه وتعالى فالحمد لله.

إيمان محمودي

Table of Contents

Chapter II: Electrical Modeling of a PV Module

ChapetrIII : Hybrid Parameters Extraction of PV Module

List of figures

Chapter I

Chapter II

Chapter III

List of Tables

Chapter I

Chapter II

Chapter III

List of symbols and abbreviations:

Ev: Energy of the valence band

Iph: Generated or photo current

V: Voltage

Vco: Open circuit voltage

Icc: Short circuit current

Iobsc: Dark current

Is: Diode saturation current

VT: Thermal potential

K: Boltzmann constant

T: Effective temperature of cells in Kelvin (K)

Rs: Series resistance

Rsh: Shunt resistance

Ta: Absolute temperature

q: Electron charge

hv: Photon energy

h: Planck constant

c: Speed of light

λ : Wavelength

Si: Silicon

Ge: Germanium

Se: Selenium

GaAs: Gallium arsenide

CdTe: Cadmium telluride

P: Power

Imp: Current at maximum power

Vmp: Voltage at maximum power

FF: Fill Factor

VcoNs: Sum of open circuit voltages of (Ns) cells in series

IccNs: Short circuit current of (Ns) cells in series

IccNp: Sum of short circuit currents of (Np) cells in parallel

Icc: Short circuit current

Vco: Open circuit voltages

VcoNp: Open circuit voltage of (Np) cells in parallel

Ns: Number of cells in series

Np: Number of cells in parallel

PV: Photovoltaic

A: Ideality factor of the junction

Pmax: Maximum power

Pi: Irradiance received per unit area (W)

S: Surface area of the photovoltaic cell (m^2)

η: Efficiency

Igl: Global radiation

Idir: Direct radiation

Idif: Diffuse radiation

ρ: Ground albedo

a and b: Coefficients representing atmospheric disturbances

dir: Total transmittance of the atmospheric layer for incident direct solar flux

ev: Electron volt

I: Current delivered by the cell (A)

Id: Diode current (A)

Tj: Junction temperature

Eg: Band gap energy of the semiconductor used

Irs: Reverse saturation current

Ipv: Current supplied by cell when operating as a generator

Vcell: Voltage across the same cell

GPV: Photovoltaic generator

G: Irradiation on the cell surface

MFO: Moth Flam Optimisation

ODM: Diode model

RMSE: Root Mean Square Error

General Introduction

General Introduction

Renewable energy is expected to be an important source of energy in the future because it replaces the depletion of the fossil fuel reserves and mitigates the pollution caused by the conventional energy sources. In particular, photovoltaic power systems could be a suitable solution to meet local energy demand. The possibility of predicting a photovoltaic array's performance in various irradiance and temperature conditions is very important for sizing the PV arrays as well as for the design of the Maximum Power Point Tracking and control strategies [1].

For this end, several research papers have focused on the modeling and parameters extraction of the PV modules as it is the key element in the energy production chain, not only to increase their performance, but also to simulate their behavior and optimize their different characteristics [2-7].

In the literature, there are two main equivalent circuit models used to describe the non-linear I–V relationship, the model with five parameters commonly called the single diode model and the one with seven parameters commonly called double diode model. Therefore, to provide an accurate modeling and reliable performance evaluation of a given solar system, a valid estimation of these model's parameters is always required. The methods employed to solve the problem of PV parameter identification can be divided in two groups; deterministic and heuristic approaches [8]. Metaheuristic algorithms are suitable choices for solving this problem due to their global search power as well as derivative-free advantage. In [9], it is stated that the heuristic algorithms give better results than classical methods in term of accuracy with a high probability to converge toward the global optimum.

In this work, a precise methodology is intended for extracting the parameters of the PV module under real operating conditions. The proposed methodology combines numerical methods and analytical formulations of the single-diode model to derive the five unknown parameters under any operating conditions of irradiance and temperature. First, the (I-V) curves measured under random weather conditions are translated to standard test conditions (i.e., G = 1000 W/m², T = 25 °C) using translation equations. The second step involves using the Moth flam optimization algorithm to identify the five parameters under standard conditions. Analytical formulations, at random irradiance and temperature, are then used to express the unknown parameters at any irradiance and temperature. The proposed approach

will be validated under outdoor conditions against the measured I-V curves in various operating conditions. Dynamic validation is also performed where the measured values of the maximum power point (MPP) coordinates are compared to the actual dynamic MPP measurements of a grid-connected system located at the Renewable Energy Development Center (CDER) in Algiers

To achieve this, we have presented this manuscript as follows: In addition to a general introduction and a general conclusion that summarizes our study, this work is divided into three chapters organized as follows:

In the first chapter, we discuss concepts related to energy and the operating principle of a silicon photovoltaic cell, as well as the different types of cells. We then address the various possible groupings of cells (PVG) and define their efficiency and fill factor.

In the second chapter, we present the mathematical modeling of the cell and the photovoltaic generator. We then use MATLAB software to initially simulate the behavior of a photovoltaic cell and then a photovoltaic generator under standard conditions. We also study the influence of temperature, irradiance, the photocurrent, the diode saturation current, the diode ideality factor and series/parallel resistance on the energy produced.

The presentation of the proposed methodology that will combine numerical methods and analytical formulations of the single-diode model to derive the five unknown parameters under any operating conditions of irradiance and temperature, as well as the obtained results, will be the focus of the third chapter.

Chapter I:

Photovoltaic System Overview

I.1 Introduction

In the contemporary world, electricity plays a pivotal role in global economic development. Its importance continues to escalate alongside advancements in technology, industrialization, and the growing desire for modern conveniences. The expansion of electricity production is synonymous with improving the quality of life and fostering economic prosperity. However, the predominant reliance on fossil fuels for electricity generation poses challenges. With the depletion of these resources, environmental apprehensions, and a notable surge in energy demand, many nations are prioritizing the quest for alternative energy sources. Renewable energies emerge as an eco-friendly substitute for fossil fuels. Their utilization holds the promise of supplying electricity on a national scale, particularly in remote regions, thereby obviating the necessity for new power infrastructure. A deeper comprehension of the significance of renewable energies, including photovoltaic energy, is imperative.

This chapter provides an overview of solar energy and its characteristics. It explains the principles of photovoltaics, the photovoltaic chain and its components, as well as the different types of photovoltaic systems.

I.4 Renewable energy potential

The International Renewable Energy Agency (IRENA) distinguishes six major sources of renewable energy (RE): biomass, geothermal, hydropower, ocean, sun and wind. Each of these sources has unique advantages and considerations, and advancements in technology continue to drive down costs and improve efficiency, making renewable energy increasingly competitive with conventional fossil fuels. As global societies work to tackle the challenges posed by climate change, renewable energy remains fundamental to decarbonizing energy systems and creating a more sustainable and equitable future for future generations. Figure (I.1) show the distribution of global energy resources in 2023[9][10]:

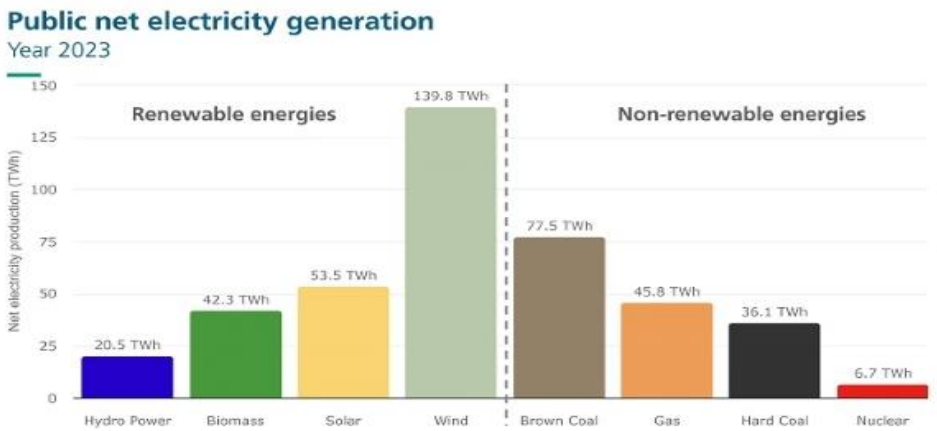

Figure (I.1): the distribution of global energy resources in 2023.

-Unlike fossil fuels (oil, coal, lignite, and natural gas), these sources are "inexhaustible" flows that regenerate indefinitely throughout time [9],[10]. In this sense, the panorama of renewable energy sources mainly consists of:

I.2.1 biomass energy

The term biomass encompasses a wide range of organic material, both plant and animal [11]. Biomass is categorized into three technical groups: wood energy (solid biomass), biogas, and biofuels. These sources are utilized to produce heat, electricity, or fuels [10]. In 2023, biomass electricity generation reached 21.6 billion kilowatt hours (kWh) and is projected to increase to 22.8 billion kWh in 2024 and 22.5 billion kWh in 2025. At that level of generation, biomass accounted for 2.47 percent of U.S. renewables generation last year and is expected to account for 2.3 percent and 2.1 percent, respectively, in 2024 and 2025[11]. Figure (I.2) explains Biomass sources.

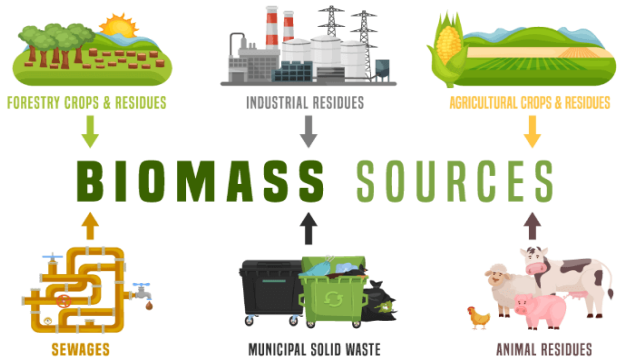

Figure (I.2): Biomass sources.

I.2.2Geothermal energy

Geothermal energy refers to the heat within the Earth, derived from the Greek words "geo" (earth) and "therme" (heat). It is considered a renewable energy source because the Earth's internal heat is continuously produced. Geothermal heat is used for bathing, heating buildings, and generating electricity [12]. The Earth's core contains an immense amount of thermal energy, some of which is accessible near the crust. Unlike many other renewable energy technologies, geothermal energy can provide continuous power. It can be harnessed from various sources, such as deep wells in Asia, hot springs in Iceland, and even in our local communities. With its low emissions, geothermal energy has the potential to significantly mitigate the effects of climate change on our planet.[13]. Figure (I.3) illustrates geothermal energy.

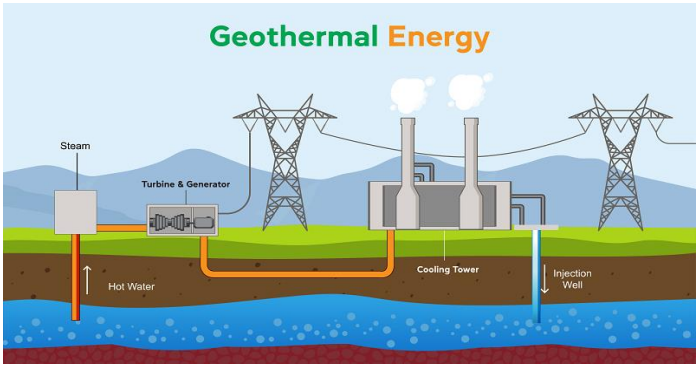

Figure (I. 3): Geothermal energy**.**

I.2.3 The hydro power Energy

Hydropower captures the energy of water moving from higher to lower elevations. It can be generated using reservoirs and rivers. Reservoir hydropower plants depend on stored water in a reservoir, while run-of-river hydropower plants utilize the flow of the river. Hydropower reservoirs often serve multiple purposes, including providing drinking water, irrigation, flood and drought control, navigation services, and energy supply. Currently, hydropower is the largest source of renewable energy in the electricity sector. Its reliability depends on stable rainfall patterns, but it can be adversely affected by climate-induced droughts or ecological changes that alter rainfall patterns [12]. Figure (I.4) show the hydro power Energy.

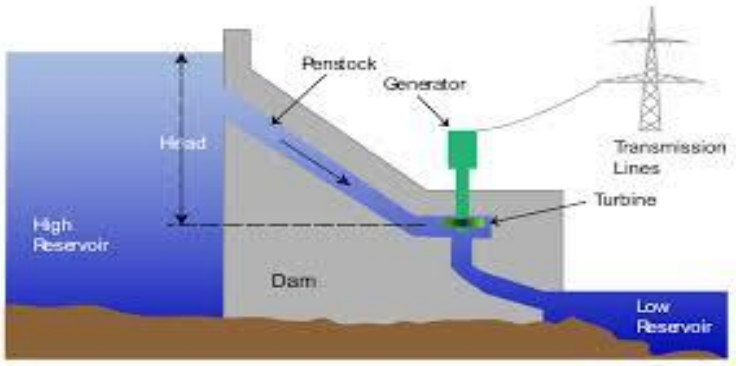

Figure (I.4): The hydro power Energy.

I.2.4 The oceans energy

The oceans contain a huge amount of energy. Capturing this energy could have substantial benefits. The energy in the ocean waves is a form of concentrated solar energy that is transferred through complex wind-wave interactions. The effects of earth's temperature variation due to solar heating, combined with a multitude of atmospheric phenomena, generate wind currents in global scale. Ocean wave generation, propagation and direction are directly related to these wind currents. Changes in salinity, thermal gradients, tidal currents or ocean waves can be used to generate electricity - and provide reliable, sustainable and cost-competitive energy [12]. Figure (I.5) explains oceans energy**:**

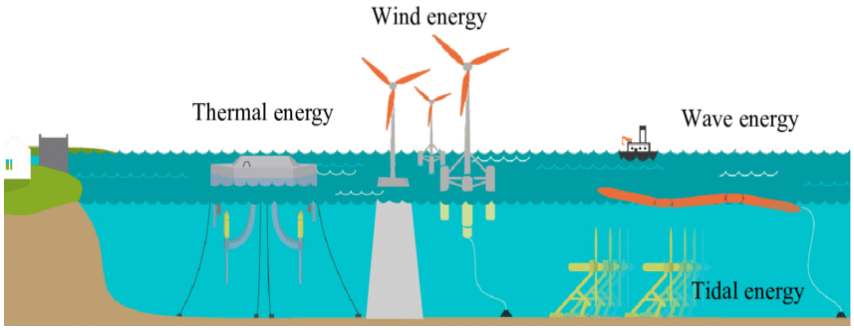

Figure (I.5): oceans energy.

I.2.5 Wind energy

Wind energy harnesses the kinetic energy of moving air using large wind turbines, which can be located on land (onshore) or in sea or freshwater (offshore). While wind energy has been utilized for thousands of years, recent advancements in onshore and offshore wind energy technologies have optimized electricity production through taller turbines and larger rotor diameters. Although average wind speeds vary significantly by location, the world's technical potential for wind energy far surpasses global electricity production, and most regions have ample potential for substantial wind energy deployment. Many areas of the world experience strong wind speeds, but the best locations for generating wind power are sometimes remote. Offshore wind power, in particular, offers tremendous potential [14]. Figure (I.6) illustrates wind energy.

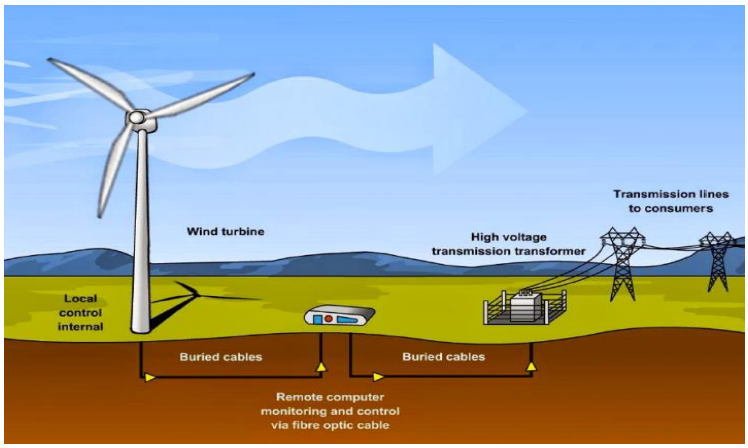

Figure (I.6): wind energy.

I.2.6 The solar energy

Solar power is energy from the sun that is converted into thermal or electrical energy. It is the cleanest and most abundant renewable energy source available, with the U.S. possessing some of the richest solar resources globally. Solar technologies can harness this energy for various purposes, including generating electricity, providing lighting or a comfortable indoor environment, and heating water for domestic, commercial, or industrial use. There are three primary methods to harness solar energy: photovoltaics, solar heating and cooling (SHC), and

concentrating solar power (CSP). Photovoltaics generate electricity directly from sunlight through an electronic process and can power anything from small devices like calculators and road signs to homes and large commercial businesses. Solar heating and cooling (SHC) systems use the sun's heat to provide space or water heating. Concentrating solar power (CSP) systems use the sun's heat to run traditional electricity-generating turbines [13]. Figure (I.7) show Sun energy.

.

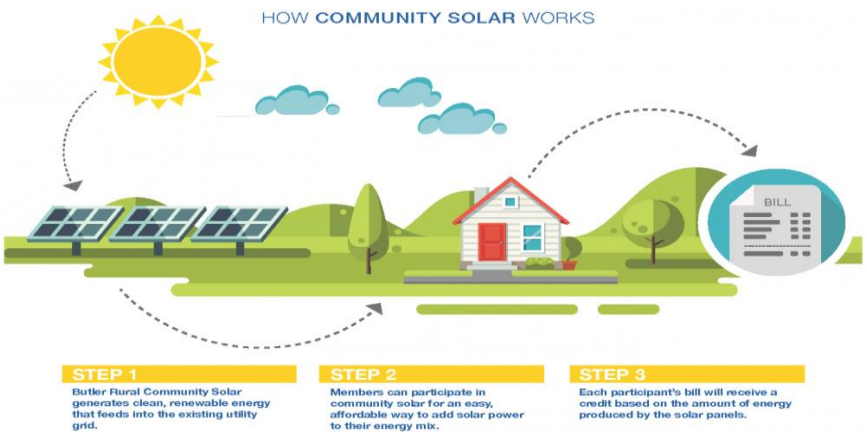

Figure (I.7): Sun energy.

I.3 Renewable energy in Algeria

Algeria's energy output is primarily defined by an overreliance on hydrocarbons (oil and natural gas), which account for 93.6% of its exports. Natural gas power stations supply over 90% of Algeria's electricity. The Algerian government is increasingly focusing on diversifying the national economy and developing new socioeconomic dynamics around renewable energies. This is primarily because Algeria has a vast potential for renewable energy resources such as solar, wind, hydro, biomass, and geothermal energy, and utilizing this potential could easily meet the country's growing energy demand while also providing a reliable source of energy exportation. Algeria has opened the road for green energy by initiating an ambitious program to promote renewable energy and energy efficiency by 2030, the initiative aims to generate 22000 MW of power from renewable energy sources. This comprises 12000 MW for local end users and 10,000 MW for export [14].

I.3.1 Solar Potential

Algeria has one of the highest solar deposits in the world due to its geographical location. The duration of sunbathing on almost the entire national territory exceeds 2000 hours annually and can reach 3900 hours (Hauts plateau et Sahara). The energy received annually on a horizontal surface of 1m2 is close to 3 Kwh/m2 in the north and exceeds 5.6 KWh /m in the Great South [10]. Figures (I.8) explains Solar Potential in Algeria:

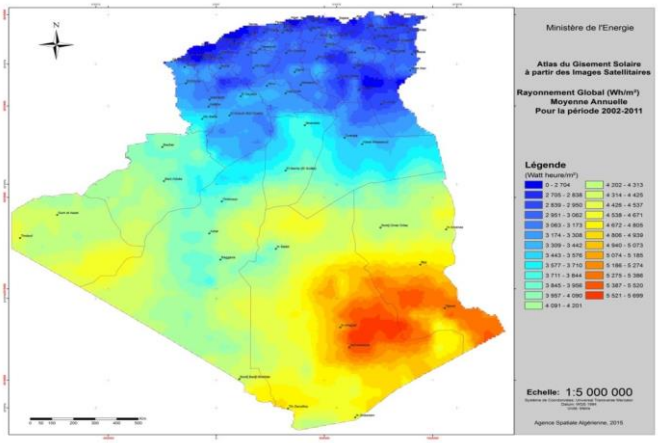

Figure (I.8): Global Direct Average Annual Irradiation Map (Period 2002-2011).

I.3.1.1 Photovoltaic System

Solar energy presents an alternative to conventional fossil fuels. Available in huge amount and distributed across the entire surface of the Earth, it allows for the capture of up to 1000 W/m2 in temperate zones. Whether in urban environments or in isolated locations, this energy can be captured and utilized in both thermal and electrical forms.

I.3.1.2 The photovoltaic effect

The photovoltaic effect is the phenomenon by which photovoltaic cells, or solar cells, directly convert sunlight into electricity. This process can be explained as follows: when a photon from solar radiation strikes a PV cell, its energy can be transferred to an electron within the semiconductor material of the cell. With this additional energy, the electron can then move from its normal position within the atom (from the valence band to the conduction band, crossing the band gap), creating a gap known as a hole, which contributes to the flow of current in an electrical circuit. This electron-hole pair is referred to as the photovoltaic effect.

I.4 Photovoltaic Cell

A photovoltaic cell is the smallest component of a photovoltaic installation. It is made up of semiconductor materials in which light energy is converted into electrical energy. The photovoltaic cell consists of a thin semiconductor layer (a material with a bandgap, which acts as an energy barrier that electrons cannot cross without external excitation, and whose electronic properties can be varied) such as silicon, which is a material with relatively good electrical conductivity, an anti-reflective layer allowing maximum penetration of solar rays, a conductive grid on the top or cathode, and a conductive metal on the bottom or anode [15]. (Figure (I.9))

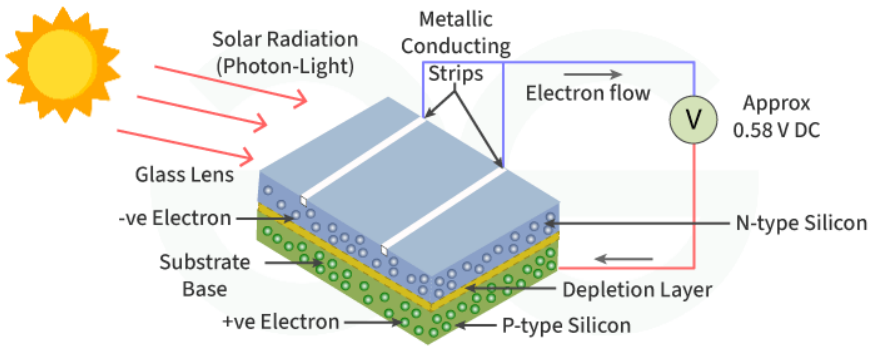

Figure (I.9): Photovoltaic Cell.

I.4.1 Principle of operation of a cell

The photovoltaic cell, found within both solar panels and the broader solar system, serves as the nucleus of electricity production through the photoelectric effect. Comprised of semiconductor materials, either singular or compound, this cell converts solar radiation into electrical energy via three fundamental mechanisms:

1. The absorption of solar radiation (or phonons) by the cell's material, necessitating that the absorbed photon energy exceeds the band gap energy Eph = hϑ.

2. The conversion of photon energy into electrical energy, achieved through the creation of electron holes.

3. The gathering of generated charges within the device through an electrical circuit.

-Operating on semiconductor principles and p-n junctions, these cells rely on materials featuring a band gap (Eg) between their valence (BV) and conduction (BC) bands, with the Fermi level situated within this gap. This Fermi level dictates the predominant charge carriers. In n-type semiconductors, electrons dominate, with the Fermi level near the conduction band, while in p-type semiconductors, electron holes predominate, with the Fermi level closer to the valence band. When p and n regions connect, a space charge or depletion region arises, fostering a permanent electric field. This results in Fermi level alignment, inducing band diagram curvature and establishing a potential barrier at the interface. A p-n junction emerges from a p-type and n-type semiconductor connection, termed a homojunction when both semiconductors are of identical material and a heterojunction when they differ [15][16]. Figure (I.10**)** explains Principle of operation of a cell:

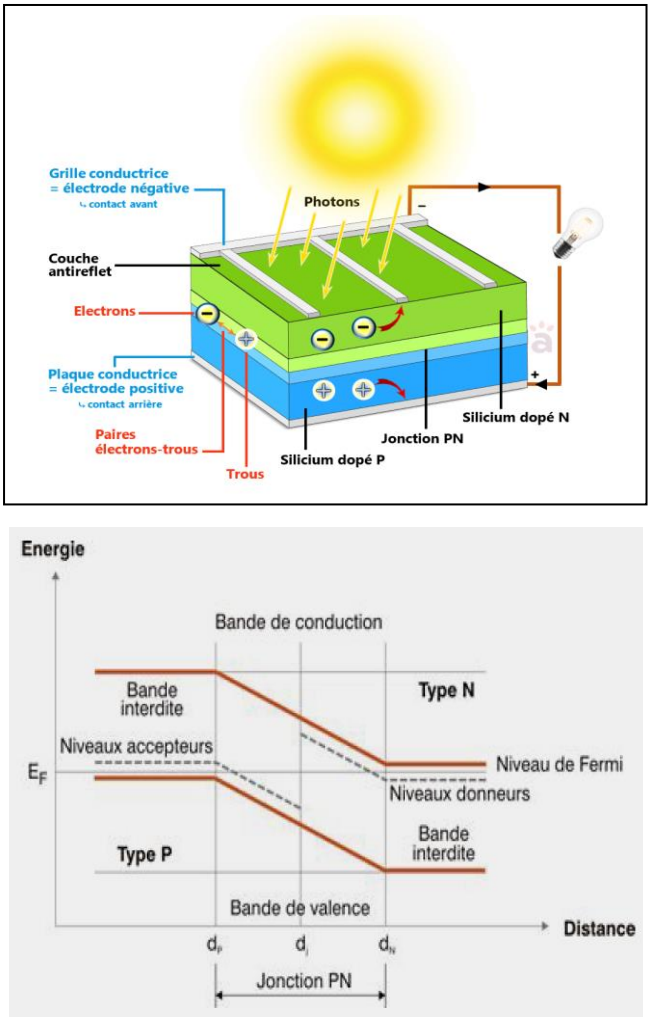

Figure (I.10): Principle of operation of a cell.

I.4.2 Type of photovoltaic cells

The cells are assembled into modules or panels: their number determines the size of the latter. To protect them from the weather, they are sandwiched between two plates of tempered glass. There are two types of solar cells. The majority (90%) of models in use consist of crystalline silicon wafers. Known as "monocrystalline" or "polycrystalline," depending on the manufacturing method, they measure 0.2 millimeters in thickness. More discreet, the "thin-film" cells are only 0.01 millimeters thick. Their main advantage is their manufacturing cost. However, their drawback is a lower efficiency, requiring an increased capturing surface to achieve power equivalent to that of crystalline cells. Indeed, the most commonly used solar cells rely on silicon, and they are classified into three types in the following table (1.2) [17]:

Cells and Modules	Characteristics	Advantages and Disadvantages	Usage
Monocrystalline Silicon 	➢ Very good efficiency: 14 to 20%. ➢ Power: 100 to 150 Wp/m². 7 m²/kWp. ➢ Long lifespan: significant (30 years).	➢ Widely available raw material. ➢ Low efficiency under low illumination. ➢ Decrease in efficiency with temperature rise. ➢ High manufacturing cost.	➢ Low-power devices. ➢ Space applications.
Polycrystalline Silicon 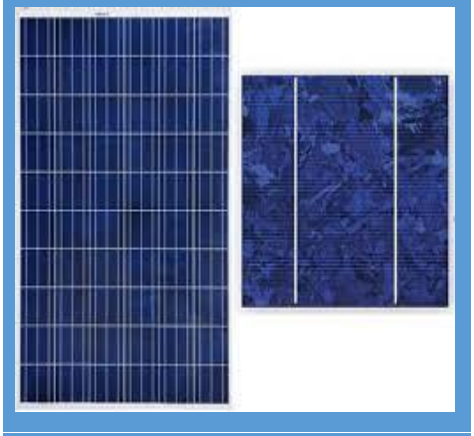	➢ Good efficiency: 11 to 15%. ➢ Power: 100 Wp/m². 8 m²/kWp. ➢ Lifespan: significant (30years) for monocrystalline.	➢ Low efficiency under low illumination and low in full sunlight. ➢ Decrease in efficiency with temperature rise. ➢ Manufacturing cost: cheaper than panels.	➢ Generators of all sizes (connected to the grid or in isolated sites).
Amorphous Silicon 	➢ Low efficiency: 5 to 9%. ➢ Power: 50 Wp/m². 16 m²/kWp. ➢ Lifespan: fairly significant (20 years).	➢ Operation under low illumination. ➢ Low efficiency. ➢ Not very sensitive to high temperatures. ➢ Manufacturing cost: inexpensive.	➢ Low-power devices. ➢ Energy production (calculators and solar watches).

Table (I.1): Type of photovoltaic cells [17].

I.5 Photovoltaic generator

Connecting several PV cells in series/parallel forms a GPV array. When cells are connected in series, their voltages add up, increasing the total voltage of the generator. Conversely, if cells are connected in parallel, it is the amperage that increases [18][19]. Figure (I.11) show Photovoltaic generator.

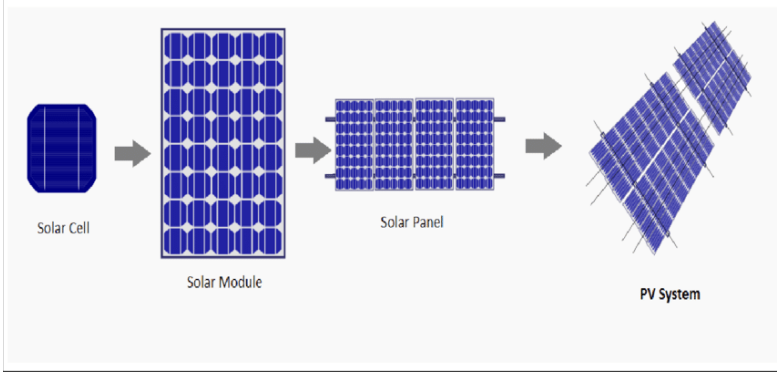

Figure (I.11): Photovoltaic generator.

I.5.1 Operating regions of the solar module

The inherent feature of the photovoltaic generator, given specific irradiance and temperature conditions, does not dictate either the current or the operating voltage; only the I(V) curve is predetermined. The load value at the terminals of the generator is what determines the operational point of the photovoltaic system. Illustrated in figure (I.12) are three crucial regions:

- Region (I): Here, the current remains consistent regardless of voltage fluctuations, indicating the photovoltaic generator functions akin to a current source.
- Region (II): This area corresponds to the characteristic's knee, serving as the intermediate region between the preceding zones and representing the optimal operating region of the generator, where the maximum power point can be identified.
- Region (III): Notable for its current variation corresponding to nearly constant voltage, in this scenario, the generator behaves akin to a voltage source [18][20].

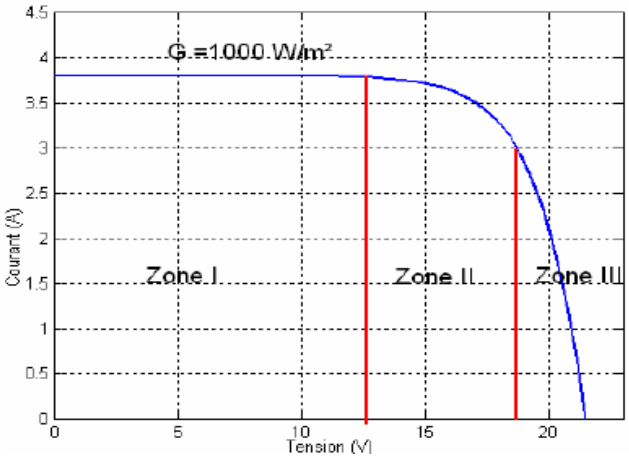

Figure (I.12): The different zones of characteristic I (V), T=25°C [18].

I.5.2 Association of photovoltaic modules

Modules can also be linked in series or parallel to augment both voltage and current intensity during operation. Nevertheless, caution is necessary as the existence of less efficient cells or shading affecting one or more cells (caused by shading, dust, etc.) could result in permanent damage to the cells. [18]

I.5.2.1 Series connection

The individual cell, which serves as the fundamental unit of a photovoltaic system, typically generates very low electrical power, usually around 0.5 W with a voltage of less than one volt. To increase power output, cells are grouped together to form a module (or panel). When cells are connected in series, the resulting voltage is the sum of the individual voltages, while the current remains equivalent to that of a single cell [18][21]**.** Figure (I.13) explains Characteristic resulting from the grouping of Ns cells in series.

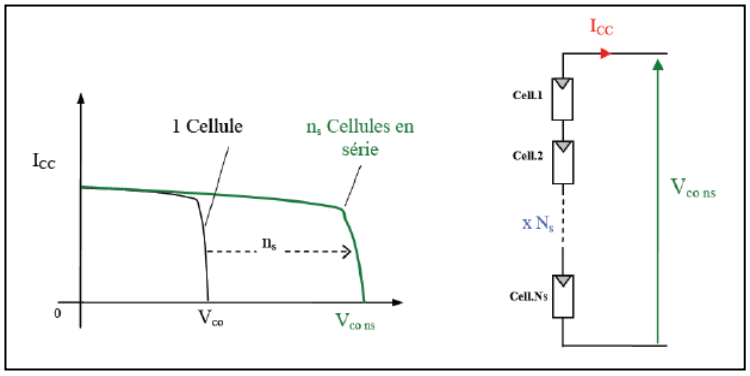

Figure (I.13): Characteristic resulting from the grouping of Ns cells in series.

I.5.2.2 Parallel connection

When identical modules are connected in parallel, the voltage across the branch equals the voltage of each module, while the current increases proportionally with the number of modules in parallel in the branch. [18][22]. Figure (I.14) show Characteristic resulting from the grouping of Ns cells in Parallel.

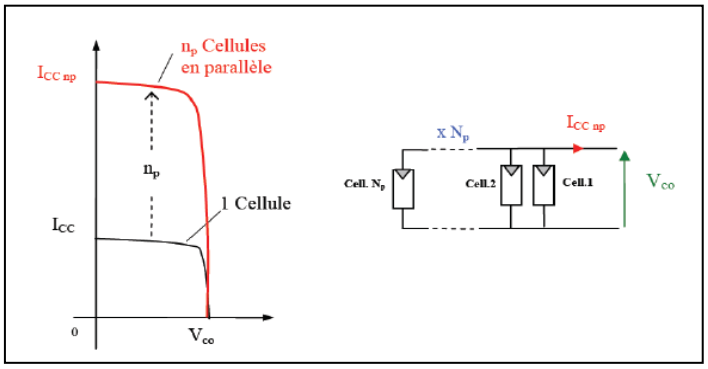

Figure (I.14): Characteristic resulting from the grouping of Ns cells in Parallel.

I.5.2.3 Série-parallel association

To achieve both current and voltage satisfaction, it is necessary to use a mixed configuration, namely Series-Parallel [18][23]. Figure (I.15) illustrates Characteristic resulting from the grouping of Ns cells in Série-parallel.

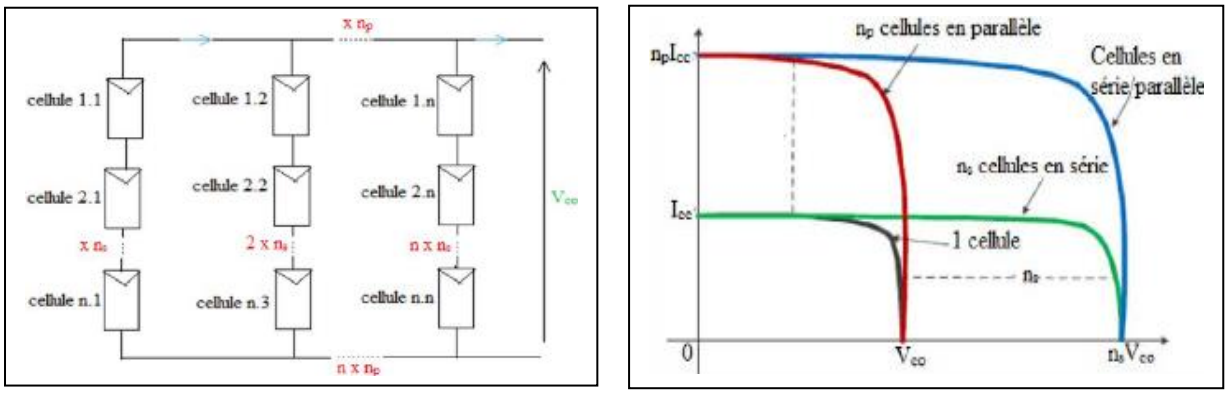

Figure (I.15): Characteristic resulting from the grouping of Ns cells in Série-parallel.

I.6 DC-DC converter (The chopper)

The DC/DC converter aims to ensure the flow of energy between a continuous voltage source and a continuous current source. It adjusts the output parameter values. If the output voltage is lower than the applied input voltage, the chopper is termed as a buck converter. Conversely, if the output voltage is higher, it is termed as a boost converter. They consist of capacitors, inductors, and switches. In the ideal case, all these devices consume no power, which is why choppers have high efficiencies

A control device, by a PWM (Pulse Width Modulation) or SPWM (Sinusoidal Pulse Width Modulation) signal, needs to be integrated into the converter's control circuit. The latter must be capable of operating the photovoltaic panel at its maximum power with a fixed switching frequency FS and a variable duty cycle α [18][24]. Figure (I.16) explains DC-DC converter (The chopper).

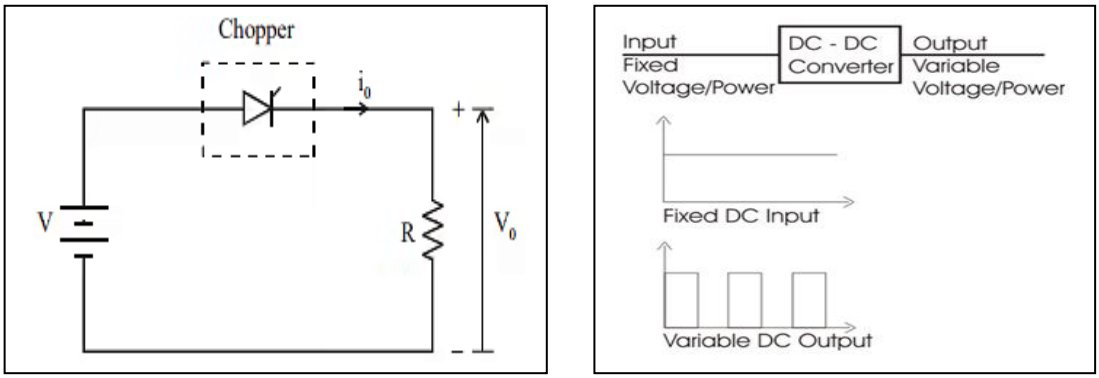

Figure (I.16): DC-DC converter (The chopper).

I.7 Types of DC-DC converters

These topologies are further classified into two main categories:

- Buck converters.
- Boost converters.

I.7.1 Buck converter

The same approach is taken in the study of the Buck converter. Figure (I.17) illustrates the structure and waveforms of the current and voltage of this converter, characterized by the series arrangement of the switch with the source. The average output voltage, the ripple current in the inductance, and the ripple of the output voltage are respectively given by [24]:

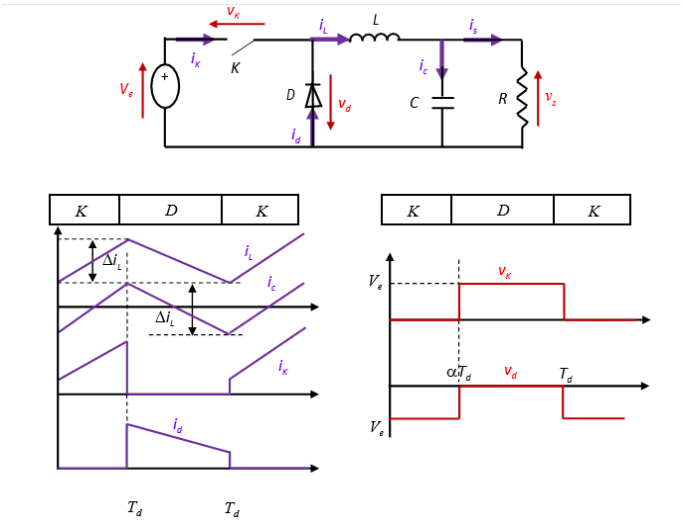

Figure (I.17): Waveforms of currents and voltages for the Buck converter [24].

I.7.2 Boost converters

Boost DC-DC converter, primarily consisting of a switch denoted as K (like an IGBT or MOSFET) and a diode labelled as D. Control of switch K is managed via a pulse width modulation (PWM) signal featuring a consistent switching period Td and an adjustable duty cycle α. The operation of both switches is complementary: when K is activated, D is deactivated, and vice versa. K remains activated throughout each cycle from time 0 to αTd. There are two discernible operational modes based on whether the inductor current reaches zero (discontinuous conduction) or not (continuous conduction). Our focus is primarily on the latter mode, deemed most significant. Figure (I.18) provides an outline of this converter's fundamental schematic, depicting the switch and diode conduction intervals, alongside the respective waveforms of their currents (left side) and voltages (right side) [24].

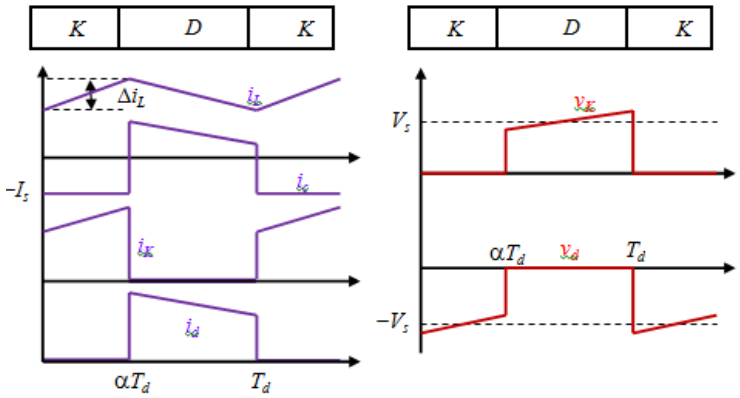

Figure (I.18): Waveforms of currents and voltages for the Boost converter [24].

➢ When the switch K is closed (0 < t < αTd), the converter circuit becomes:

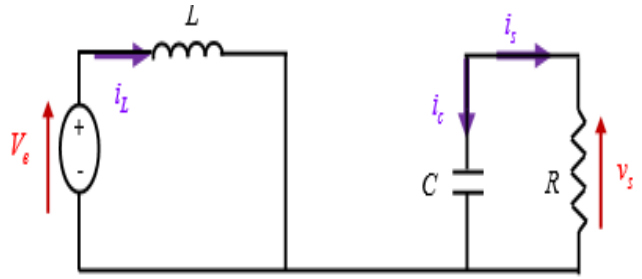

Figure (I.19): Equivalent circuit of the Boost converter when the switch is closed [24].

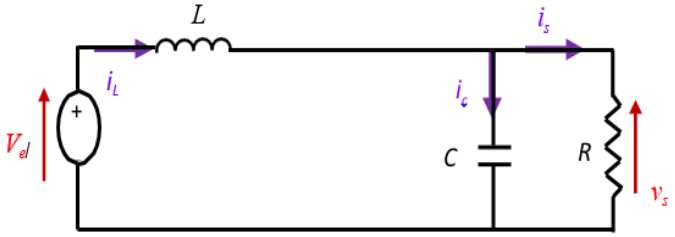

Figure (I.20): Equivalent circuit of the Boost converter when the switch is open. [24].

- The converter's output voltage can be controlled by adjusting either its input voltage or its duty cycle, with the duty cycle ranging between 0 and 1, making it function effectively as a voltage booster.

I.8 Conclusion

In this chapter, we examined the principle renewable energy sources. Subsequently, the photovoltaic effect is discussed, we described the constituent elements of the photovoltaic chain by defining the main parts. Next, we demonstrated the effects of connecting PV cells in series and parallel on the voltage and current at the level of a photovoltaic generator (PVG). Finally, the different types of DC/DC converted is presented. The equivalent circuit of PV solar cell and the influence of its parameters on the output power generation will be the purpose of the next chapter.

Chapter II
Electrical Modeling of a PV Module

II .1 Introduction

The modeling of photovoltaic (PV) cells involves using mathematical methods and computer simulations to represent the behavior and performance of solar cells. This approach allows predicting how a photovoltaic cell will react under different metro-logical and design conditions, which is crucial for optimizing their efficiency and utilization in solar systems [25]. This chapter explores different electrical and mathematical models that characterize photovoltaic cells and generators. We'll focus on modeling the ISOFOTON 106/12 photovoltaic generator. We'll investigate how temperature and illumination affect, as well as the impact of different modeling parameters on the energy output of the photovoltaic module.

II .2 Equivalent circuit of a solar cell

II .2.1Cas of an ideal cell

It is called the ideal model. It is the simplest model to represent the solar cell, as it only takes into account the diffusion phenomenon. The simplified equivalent circuit of a solar cell consists of a diode and a current source connected in parallel. The current source produces the photon current Iph, which is directly proportional to the solar irradiance G [26].Figure (II.1) show Equivalent circuit of an ideal

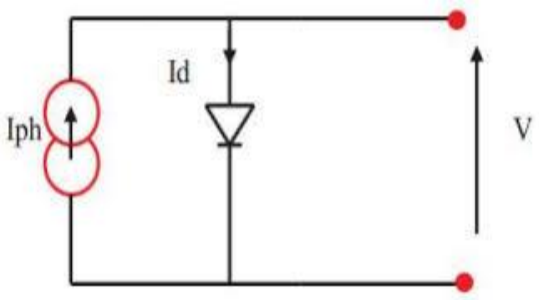

Figure (II.1): Equivalent circuit of an ideal

$$I = I_{ph} - I_d \quad \text{(II.1)}$$

With:

I: Current delivered by cell (A)

Iph: Short circuit current (A)

Id: current in the diode (A)

- The characteristic IV of a diode is a nonlinear characteristic given by the relation:

$$Id = Is\left(e^{\frac{Vd}{Vt}} - 1\right) \quad \text{(II.2)}$$

$$I = I_{ph} - I_d = I_{ph} - Is\left(e^{\frac{Vd}{Vt}} - 1\right) \quad \text{(II.3)}$$

Vt = A.K.Tj/q: thermal potential.

K: the Boltzmann constant is equal to 1.38e-38J/K.

A: ideal junction factor Tj: junction temperature (°C).

Is: The Diode Saturation Current (A).

q: the charge of the electron is equal to 1.610e-19.

V: voltage delivered by the cell (V).

Vd: voltage at the diode ends (V).

II .2.2 Cas of a real cell

Figure (II.2) depicts the corresponding pattern of the real photovoltaic cell, which accounts for manufacturing-related parasitic resistance effects. This equivalent scheme is made up of a shunt resistor (R_{sh}), which characterizes a leak current between the upper grid and the rear contact that is typically much greater than (R_S); a diode (d) characterizes the junction; a current source (I_{ph}) characterizes the photo-current; and a serial resistance (Rs) represents the Joule-effect losses, This model is claimed to include five parameters, which are: photocurrent (I_{ph}), saturation current (I_0), junction idealist factor (A), serial resistance (Rs), and shunt resistance. The five-parameter model provides a nice balance of simplicity and accuracy. These equations define the I-V characteristics of the cell and module by providing formulas for the various currents [26].

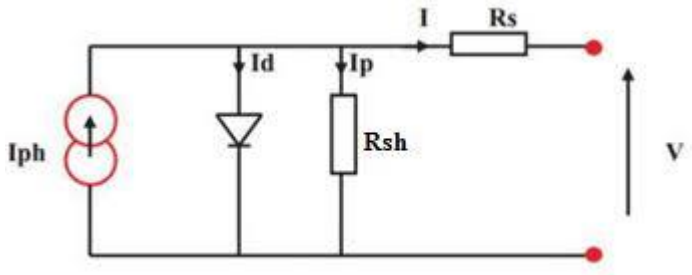

Figure (II.2): Equivalent circuit of a real cell

$$I = I_{ph} - I_d - I_{sh} \quad \text{..... (II.4)}$$

With:

$$I_{sh} = \frac{V_d}{R_{sh}} = \frac{V+RsI}{R_{sh}} \quad \text{..... (II.5)}$$

Hence the current equation given by the following expression:

$$I = I_{ph} - I_d = I_{ph} - I_0\left(e^{\frac{Vd}{Vt}} - 1\right) - \frac{V+RsI}{R_{sh}} \quad \text{.....(II.6)}$$

With:

Iph: The photonic current, it depends on temperature and sunlight as shown in the following equation:

$$Iph = [Icc + Ki\,(T - Tref)] * \frac{E}{1000} \quad \text{..... (II.7)}$$

$\boldsymbol{I_{ph}}$: is in [A], calculated under nominal conditions (25° and 1000 W/m²).

$\mathbf{K_i}$: is the ratio between the short-circuit current and the temperature coefficient (0.0017 A/K).

$\boldsymbol{T_{ref}}$: Reference temperature, equal to 25°C.

$\boldsymbol{I_{cc}}$: short-circuit current.

$\boldsymbol{I_0}$: is the saturation current expressed as:

$$I_0 = I_{r_s}.\left[\frac{T}{Tref}\right]^3 exp\left[\frac{q.Eg}{A.K}.\left\{\frac{1}{Tref}-\frac{1}{T}\right\}\right] \text{ …….. (II.8)}$$

E_g: The energy gap of the semiconductor used ($Eg \approx 1.1$ eV for polycrystalline silicon at 25°C).

I_{rs}: the reverse saturation current, which is given by:

$$Irs = \frac{Icc}{[\exp(\frac{q.Voc}{K.A.T})-1]} \text{.....(II.9)}$$

q: The charge of the electron, equal to 1.6 * 10^{-19} C.

K: Boltzmann constant, equal to 1.3805 * 10^{-23} J/K.

A: Ideality factor, equal to 1.6.

-To calculate the short-circuit voltage, we solve the equation:

$$Vco = \frac{K.T}{q}.ln(\frac{Icc}{Is}-1) \text{..... (II.10)}$$

- Thus, the overall equation modeling the photovoltaic generator is as follows:

$$I_{PV} = N_p I_{ph} - N_p I_S\left[\exp\left(\frac{q(V_{cell}+R_S I_{cell})}{N_S AKT}\right)-1\right] - N_p\frac{V_{cell}+R_S I_{cell}}{R_{sh}} \text{.....(II.11)}$$

Where:

I_{pv}:is the current provided by the cell when it operates as a generator.

T: is the effective temperature of the cells in Kelvin (K).

V_{cell}: is the voltage across this same cell.

R_{sh}: is the shunt resistance characterizing the leakage currents of the junction.

R_s: is the series resistance representing the various contact and connection resistances.

II .3 Photovoltaic Module GPV and Its Performance

In a photovoltaic solar power plant, the photovoltaic field comprises several solar panels (modules). Thus, each solar panel is made up of multiple PV cells connected in series, parallel, or series-parallel configurations to form the photovoltaic module. Figure (II.3) presents actual photographs of a cell, a panel, and a photovoltaic field [27].

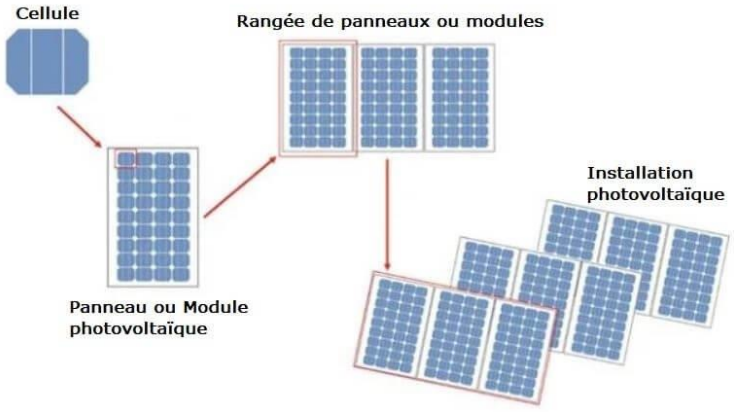

Figure (II.3): Photovoltaic Cell, Module, and Panel.

II .3.1Grouping of Photovoltaic Cells

Since the power generated by a single solar cell is very low, multiple cells with similar characteristics need to be electrically connected and encapsulated in plastic to form a practical PV module [28]. The following sections describe the different possible configurations for connecting solar cells.

II .3.2 Influence of the series connection of PV cells

The series association of Ns cells with the same current amplifies the voltage within the photovoltaic generator. The resultant trait of the series arrangement is achieved by accumulating the individual voltages of each cell. Therefore, the current in the PV generator is equivalent to that of a single cell, while the output voltage is increased (due to the summation of voltages from all cells). [22]. The equation encapsulating the electrical feature of the series association of Ns cells is as follows:

$$VPV=NS*Vco \quad \text{(II.12)}$$

$$IPV=Icc \quad \text{(II.13)}$$

With:

NS: number of cells in series.

Icc: short-circuit current (A).

Vco: Open-circuit voltage.

The characteristic of a series grouping of solar modules is represented by Figure (II.4):

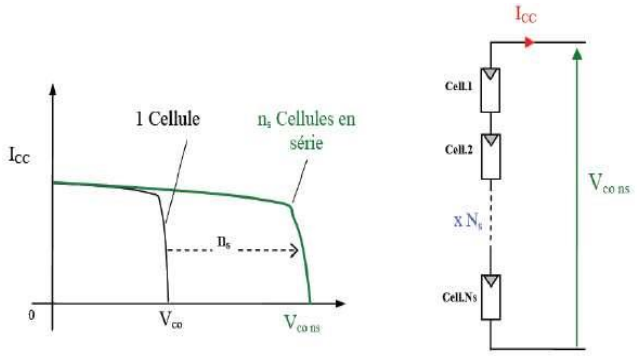

Figure (II.4): Current-voltage characteristic of NS cells in series.

II .3.3Influence of the parallel association of PV cells

A parallel association enhances the output current of the generated generator. When identical cells are connected in parallel, they experience the same voltage, and the resultant characteristic of the grouping is obtained by summing the currents. Equations (II.14) and (II.15) along with Figure (II.5) summarize the electrical features of a parallel association comprising (NT) cells [27].

$$IPV=NP*Icc \quad \text{(II.14)}$$

$$VPV=Vco \quad \text{(II.15)}$$

With:

NP: Numbers of cells in parallel

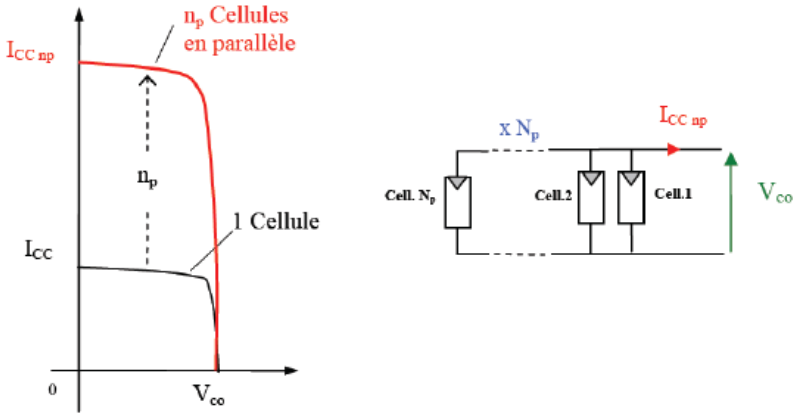

Figure (II.5): Current-voltage characteristic of NS cells in parallel.

II.4 Simulation of a Photovoltaic Cell

The electrical characteristics of the cell are given in the following table:

Parameter	Value
Standard Irradiance (G)	**1000 W/m²**
Standard Temperature (T)	**25°C**
Ideality Factor (A)	**1.3**
Band Gap Energy (Eg)	**1.12 eV**
Short-Circuit Current (Isc)	**7.35 A**

Table (II.1): Electrical characteristics of the cell under standard conditions (STC): T=25°C, G=1000 W/m² [18].

II.4.1 I(V) and P(V) Characteristics

The results from the simulation of the current-voltage (I(V)) and power-voltage (P(V)) characteristics of the photovoltaic cell under standard conditions (T=25°C, E=1000 W/m²) are shown in figures (II.7) and (II.8).

- Figure (II.7) illustrates the current-voltage characteristic of a solar cell under conditions of E=1000 W/m² and T=25°C. The short-circuit current is 7.35 A, and the open-circuit voltage is 0.6 V.
- It can be observed that the I(V) characteristic of a photovoltaic cell resembles that of a P-N junction diode in reverse bias, but it is shifted along the current axis by an amount directly proportional to the irradiance.

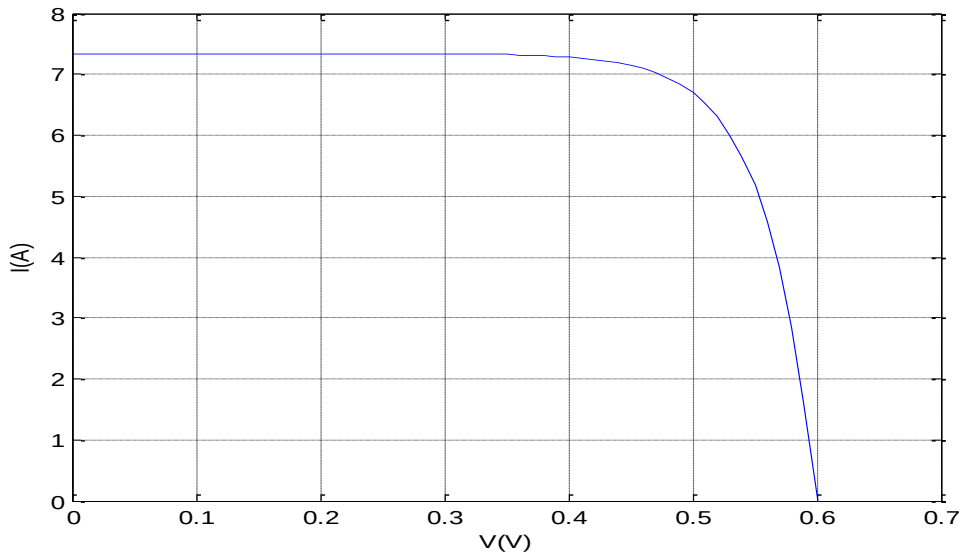

Figure (II.6): The I(V) characteristic of a cell (T=25°C, G=1000W/m²).

- Figure (II.8) shows the power-voltage characteristic of a solar cell under conditions of G = 1000 W/m² and T = 25°C. It can be observed that as the voltage increases, the power increases up to the optimal value (Pmax), after which it decreases, the short-circuit current is Isc = 4.14A, and the open-circuit voltage is Voc = 21.6V:

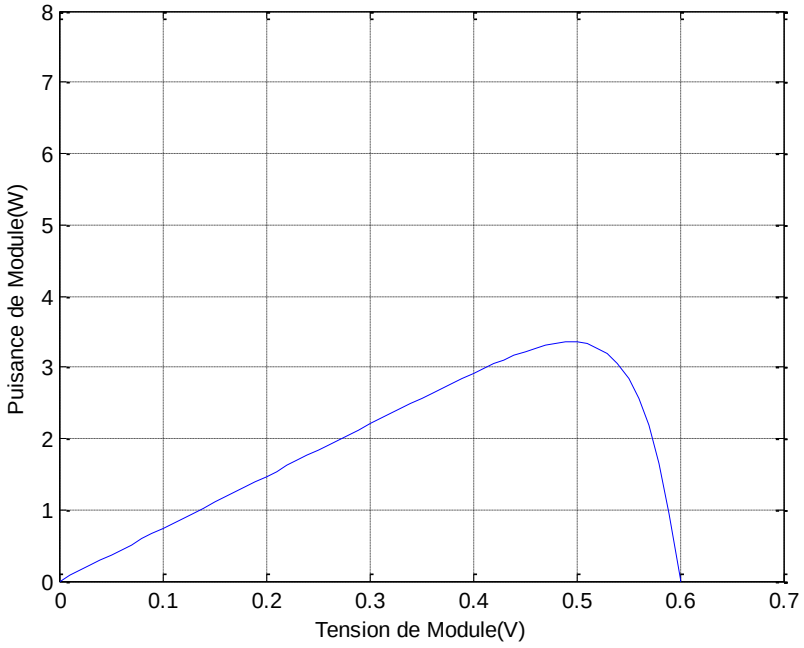

.

Figure (II.7): The P(V) characteristic of a cell (T=25°C, G=1000W/m²).

II.5 Simulation of a Photovoltaic Generator

The collected measurement data from ISOFOTON 106/12 module has been used, where its electrical characteristic is summarized in Table (II.2):

	ISOFOTON 106/12
$P_{mp}(W)$	106
$V_{OC}(V)$	21.6
$I_{SC}(A)$	6.54
$V_{mp}(V)$	17.4
$I_{mp}(A)$	6.10
$\alpha I_{SC}(\%/°C)$	0.060
$\beta V_{OC}(\%/°C)$	-0.36

Table (II.2): Electrical Characteristics of a Photovoltaic Generator.

- Figures (II.9) and (II.10) present the Characteristics I(V) et P(V) of a Photovoltaic Generator, taking in consideration the following values parameters: R_s= 0.43Ω; R_{sh}= 66.62Ω; n= 51.17; I_{ph}= 4.09A; I_0= 4.64e-06 A

II.5.1 The Characteristics I(V)

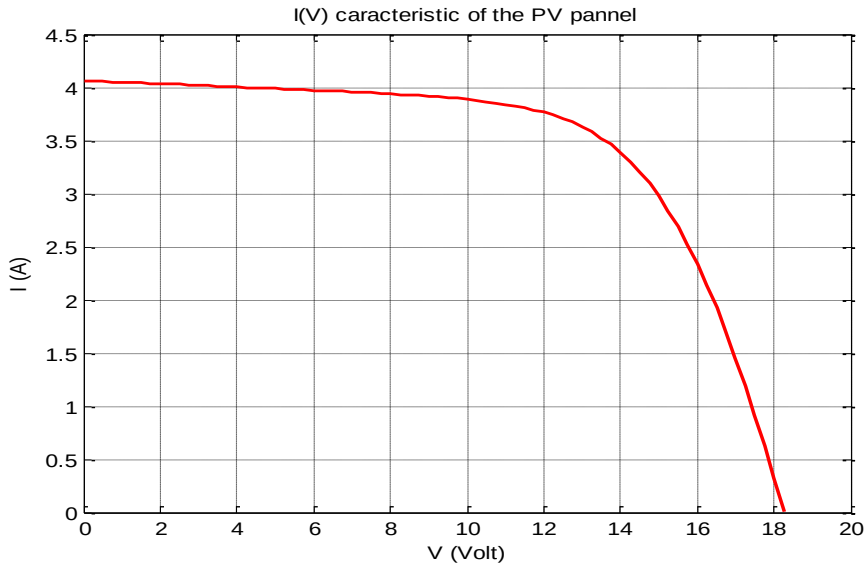

Figure (II.8): The Characteristics I(V)of a Photovoltaic Generator (T=25°C, G=1000W/m²).

II.5.2 The Characteristics P(V)

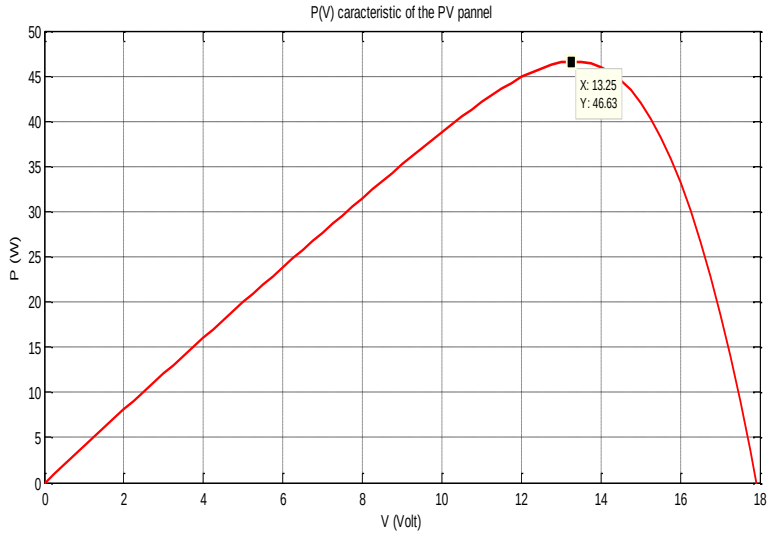

Figure (II.9): The Characteristics P(V)of a Photovoltaic Generator (T=25°C, G=1000W/m²).

- The power output of the photovoltaic generator depends on its operating point, as shown in Figure (II.9). The point "M" represents the maximum power output of the generator. At this point, Pmax = 51.7 W, which is verified by:

$$Pmax=13.25V\times3.44A=45.63W.$$

II.6 Influence of Climatic Parameters on a Photovoltaic Generator

II.6.1 Influence of Irradiance on the Photovoltaic Generator

By varying the irradiance between 600 W/m² and 1200 W/m² in steps of 200, the (I=f(V)) characteristic is shown in Figure (II.11). It can be observed that the short-circuit current is directly proportional to the irradiance intensity. However, the open-circuit voltage does not vary in the same proportions; it remains nearly constant even at lower irradiance levels.

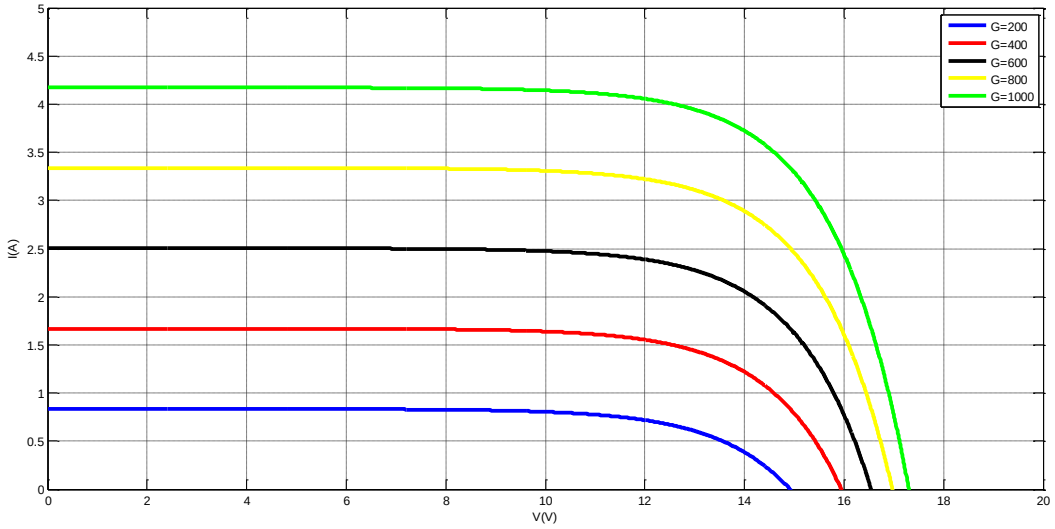

Figure (II.10): I(V) Characteristic for Different Levels of Irradiance (T=25°C).

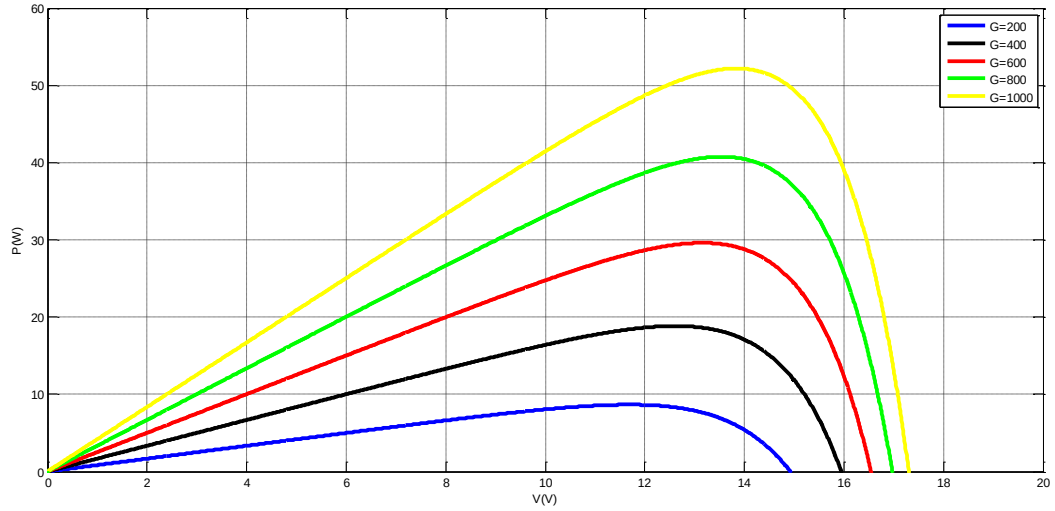

Figure (II.11) :P(V) Characteristic for Different Levels of Irradiance (T=25°C).

II.6.2 Influence of Temperature on the Generator

By varying the temperature from 25°C to 55°C under the same irradiance condition (G=1000

W/m²), the I(V) characteristic (Ipv=f(Vpv)) is shown in Figures (II.12). It can be observed that temperature has a negligible influence on the short-circuit current. However, the open-circuit voltage decreases significantly as the temperature increases, consequently reducing the extractable power, as shown in Figures (II.13). When designing an installation, it is essential to account for the temperature variations of the site.

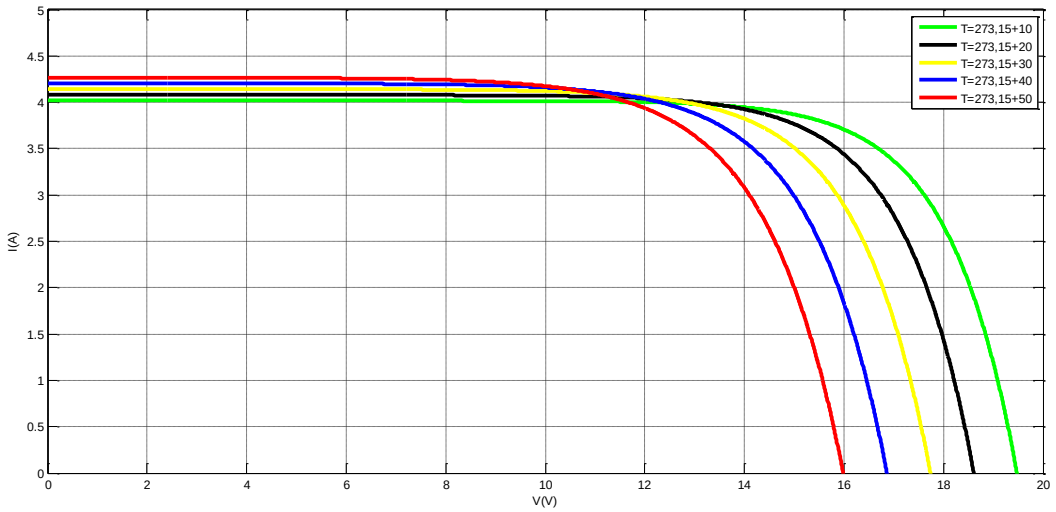

Figure (II.12): I(V)Characteristic of a Generator for Different Temperatures (G=1000W/m²).

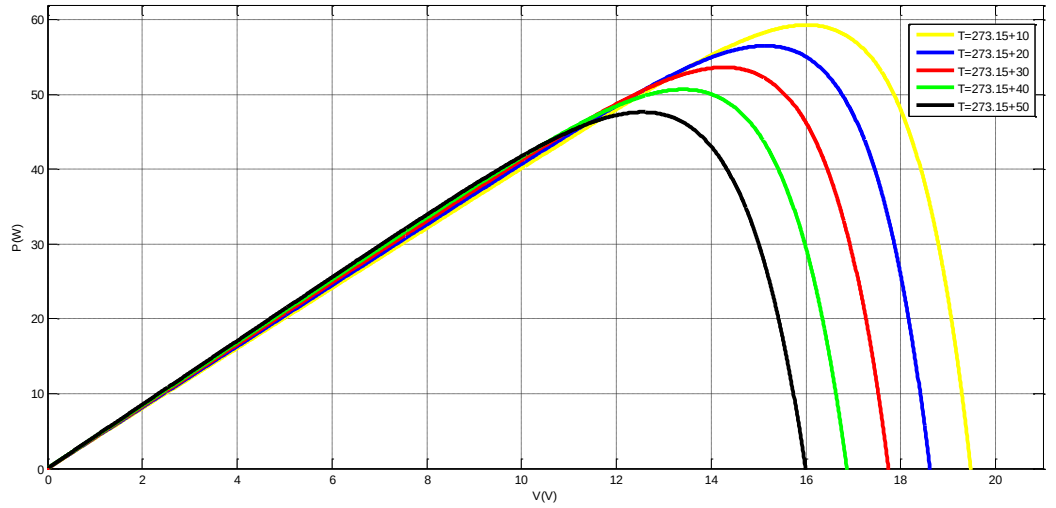

Figure (II.13): P(V) Characteristic of a Generator for Different Temperatures (G=1000W/m²).

II.7 Influence of Electrical Parameters on a Photovoltaic Generator

II.7.1 Influence of Series Resistance on a Photovoltaic Generator

The series resistance affects the slope of the characteristic in the region where the photodiode behaves as a voltage generator. When it is high, it decreases the value of the short-circuit current. Figure (II.14) illustrates the impact of the series resistance on the I(V) characteristic of the cell, resulting in a reduction in the slope of the power-voltage P(V) curve in the region where the cell functions as a constant voltage generator (Figure (II.15)).

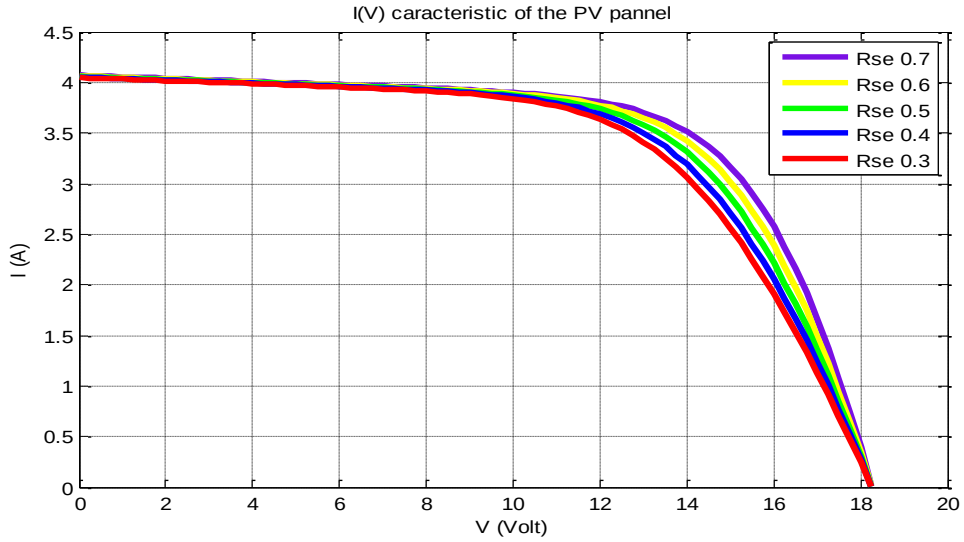

Figure (II.14): I(V) Characteristic for Different Values of Series Resistance (T=25°C), and (G=1000W/m²).

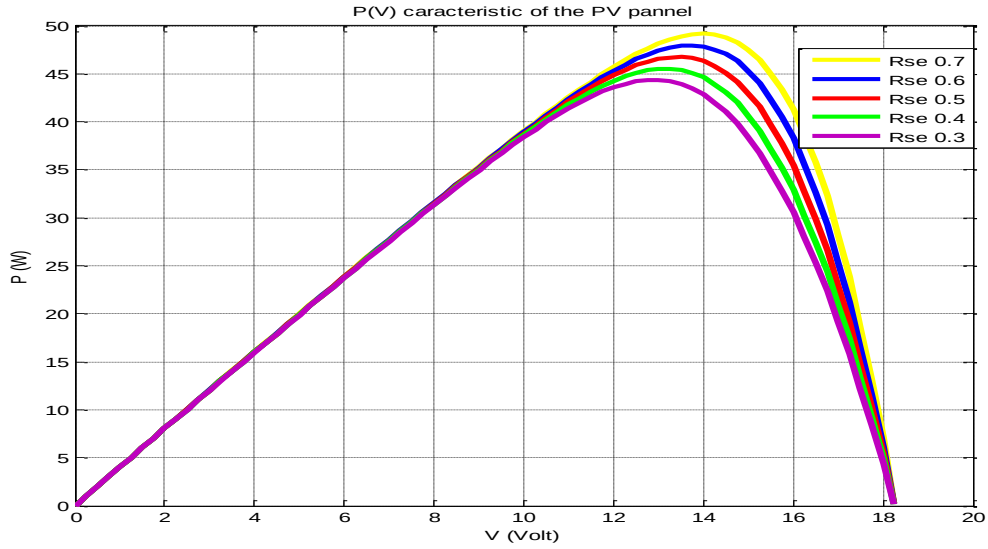

Figure (II.15): P(V) Characteristic for Different Values of Series Resistance (T=25°C), and (G=1000W/m²).

II.7.2 Influence of Shunt Resistance on the Photovoltaic Generator

The shunt resistance is directly related to the manufacturing process, and its influence becomes noticeable only for very low current values (close to the short-circuit current). As depicted in Figure (II.16) and (II.17), this influence manifests as an increase in the slope of the I(V) curve of the panel in the corresponding zone where it operates as a current source. This occurs because, in addition to the diode's forward current, an additional current linearly varying with the developed voltage must be subtracted from the photocurrent.

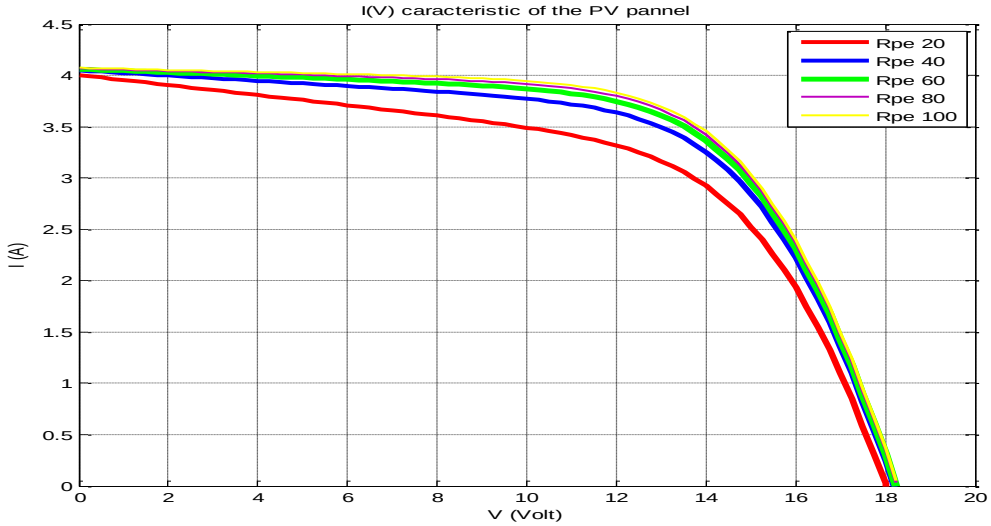

Figure (II.16): I(V) Characteristic for Different Values of Shunt Resistance (T=25°C), and (G=1000W/m²).

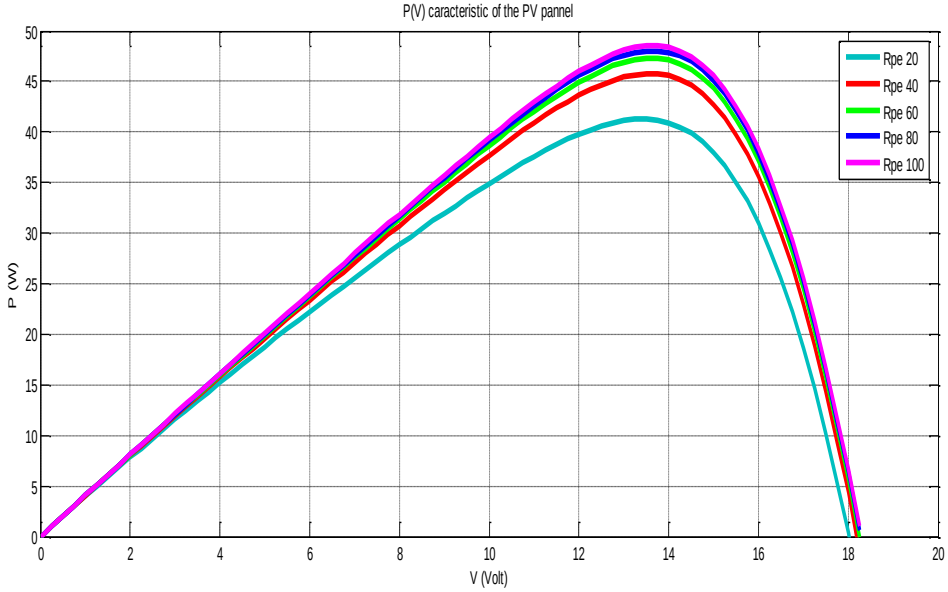

Figure (II.17) :P(V) Characteristic for Different Values of Shunt Resistance (T=25°C) and (G=1000W/m²).

II.7.3Influence of the photocurrent Iph on the Photovoltaic Generator

The photocurrent Iph is a critical parameter in the performance of a photovoltaic (PV) generator. It is the current generated by the PV cell due to the absorption of photons from sunlight. The magnitude of Iph directly affects the current-voltage I(V) and power-voltage P(V) characteristics of the PV generator (in Figure (II.18) and (II.19)):

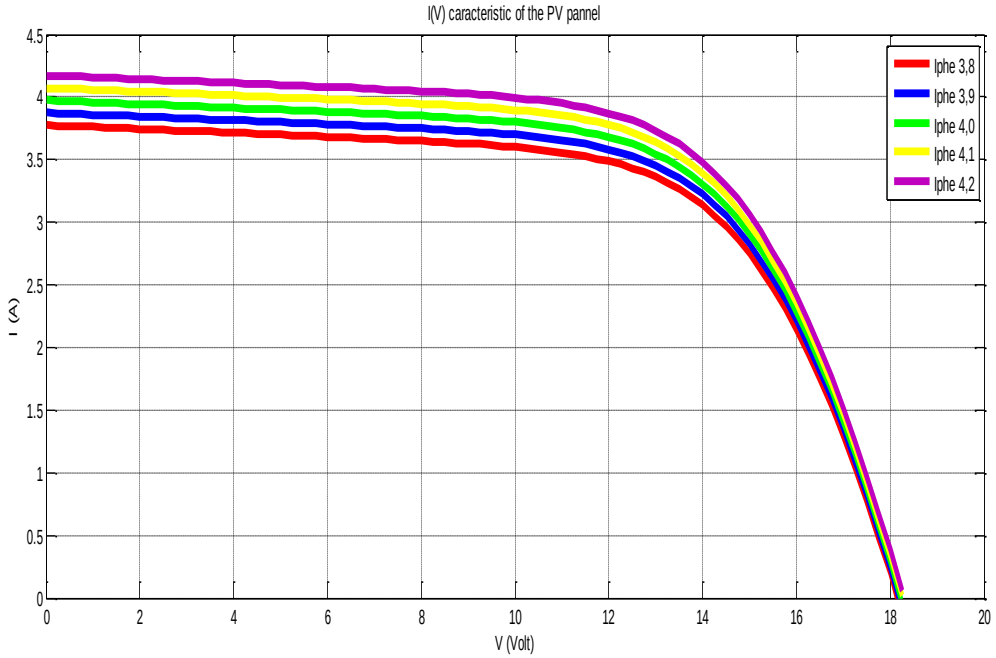

Figure (II.18): I(V) Characteristic for Different Values of Iph (T=25°C), and (G=1000W/m²).

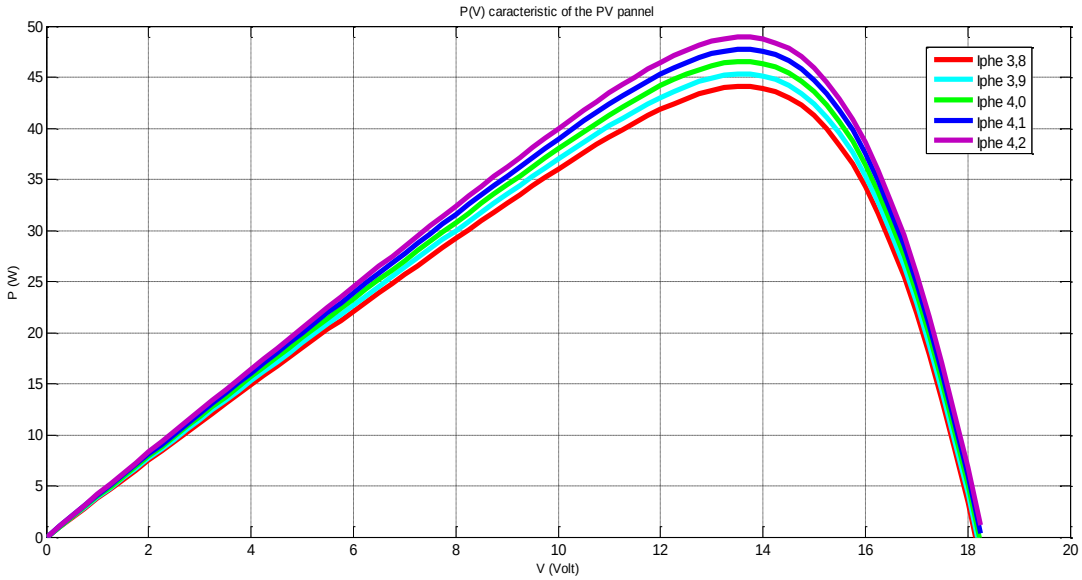

Figure (II.19): P(V) Characteristic for Different Values of Iph (T=25°C), and (G=1000W/m²).

II.7.4 Influence of current Isate on the Photovoltaic Generator

The saturation current Isate, also known as the reverse saturation current, is a crucial parameter in the performance of a photovoltaic (PV) cell. It represents the small current that flows through the PV cell when it is reverse biased. The value of Isate affects the current-voltage (I(V)) characteristics and the overall efficiency of the PV generator (in figure (II.20) and (II.21)):

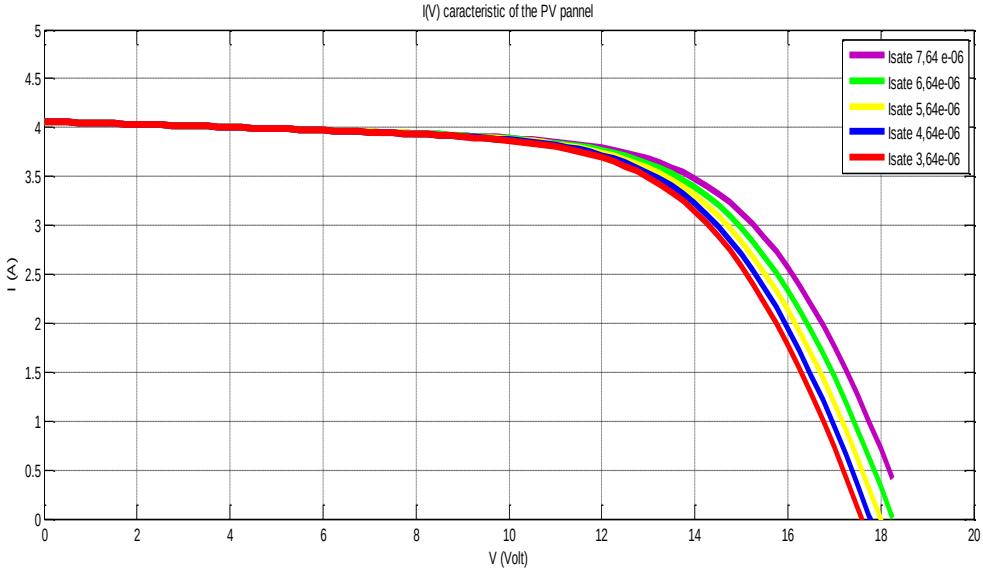

Figure (II.20): I(V) Characteristic for Different Values of Isate (T=25°C), and (G=1000W/m²).

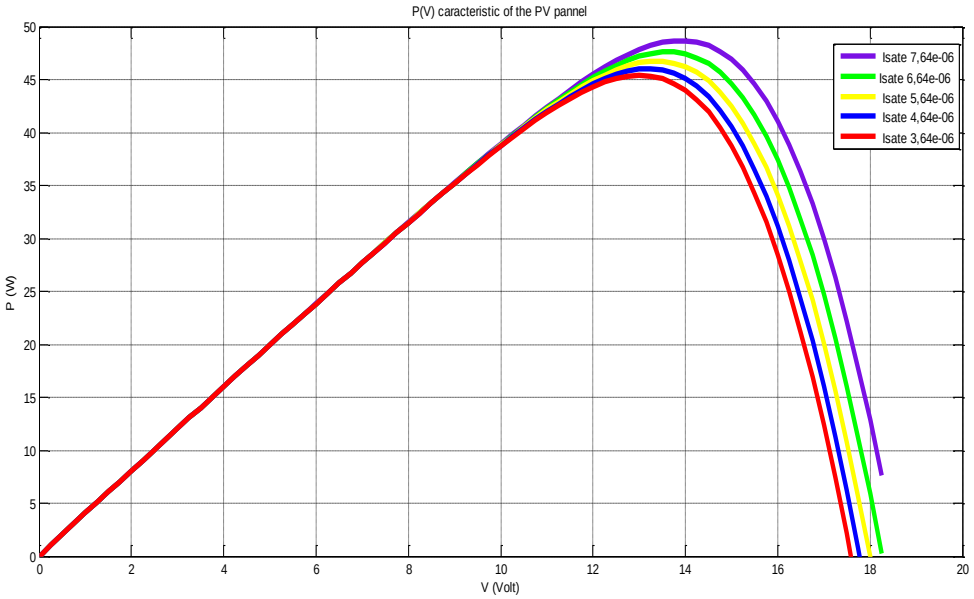

Figure (II.21): P(V) Characteristic for Different Values of Isate (T=25°C), and (G=1000W/m²).

II.7.5 Influence of ideality Factor ne on the Photovoltaic Generator

The ideality factor (n) is a parameter that indicates how closely the behavior of a diode (including a photovoltaic cell) approximates that of an ideal diode. It affects the current-voltage (I-V) characteristics and overall performance of a photovoltaic (PV) generator. Typical values of the ideality factor range between 1 (for an ideal diode) and 2(in figure (II.22) and (II.23)):

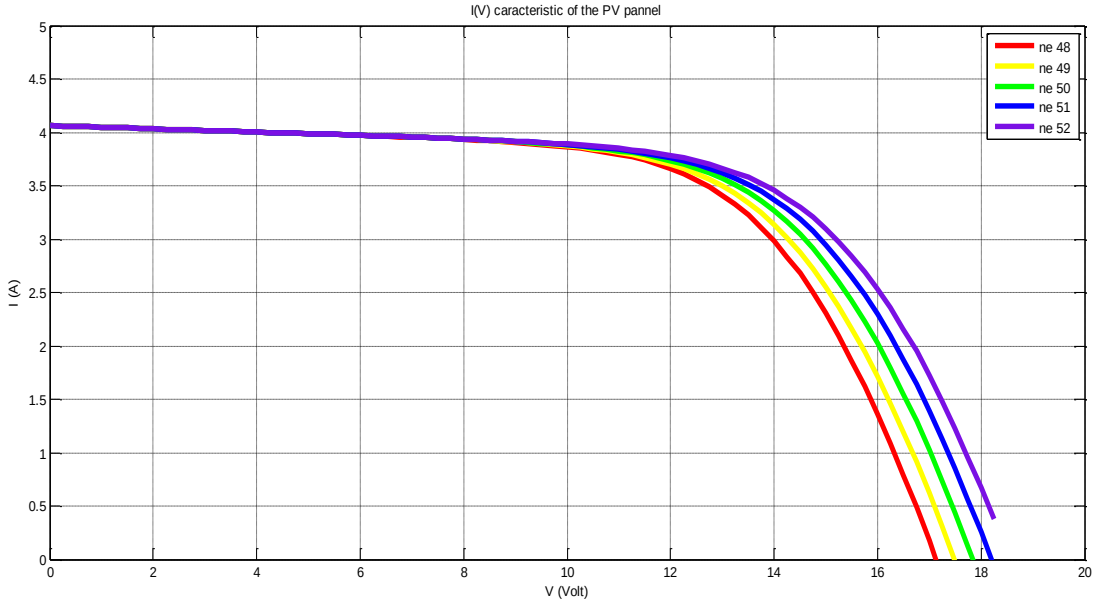

Figure (II.22): I(V) Characteristic for Different Values of ne (T=25°C), and (G=1000W/m²).

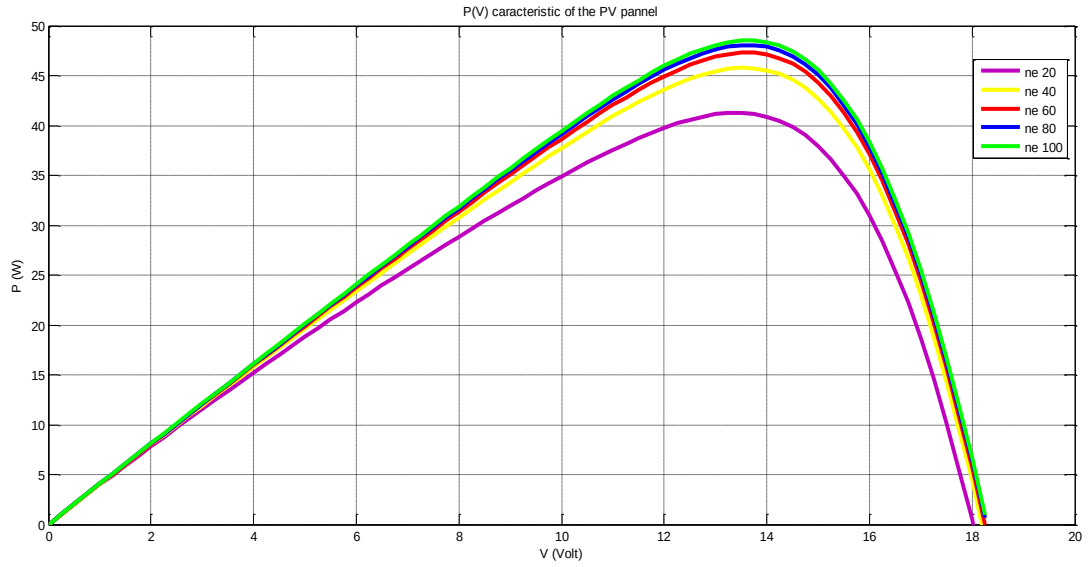

Figure (II.23): P(V) Characteristic for Different Values of ne (T=25°C), and (G=1000W/m²).

II.8 Conclusion

In this chapter, we have presented the mathematical modeling of the photovoltaic cell and generator. Subsequently, we utilized MATLAB software to initially study the behavior of an ISOFOTON 106/12 generator. We also investigated the influence of temperature, irradiance, and the impact of electrical parameters on the energy produced by the PV generator. The presentation of the precise methodology that intends for extracting the parameters of the PV module under real operating conditions will be the subject of the next chapter.

Chapter III
Hybrid Parameters Extraction of a PV Module

III.1 Introduction

The accurate characterization and prediction of current-voltage characteristics of photovoltaic (PV) modules under different operating conditions is the main step for energy prediction and an important tool for monitoring and supervision the system. However, one of the problems of this technology is that as yet there are no models in the literature to directly calculate the daily dynamic maximum power of these kinds of PV systems. The main motivation of the present chapter is to propose an accurate module parameters extraction approach that combines analytical formulation and a numerical optimization method. The suggested approach contains three primary stages. In the first stage, actual I-V curves translation to the reference conditions (i.e., G = 1000 W/m2, T = 25 °C) using analytical formulation. In the second stage, the five unknown parameters in standard conditions are extracted based on the moth flame optimization (MFO) algorithm combining the translated I-V curves with the analytical formula at the reference conditions. The last step consists to find out the I-V couples at actual conditions of temperature and irradiance based on analytical formulas and the reference parameters extracted numerically by the MFO algorithm.

III.2 Description of the experimental arrangement

To thoroughly evaluate the effectiveness of the novel method for determining the unknown parameters of the PV model, data from a grid-connected PV system in Algiers, Algeria, were utilized. Situated at coordinates 36°43'N latitude and 3°15'E longitude, this PV system has a total capacity of 9.54 kW, distributed across three sub-arrays, each with a capacity of 3.18 kW. Each sub-array consists of 30 ISOFOTON106-12 panels arranged in two parallel strings of 15 modules in series (Figure III.1).

These PV modules are linked to a 2.5 kW single-phase inverter (IG30 Fronius).

Figure (III.1): The PV system diagram

The PV plant's inclined and flat solar radiation levels are observed with a *Kipp &Zonen*CM11 thermoelectric pyranometer. Temperature readings of the PV panels are also taken using K-type thermocouples. Meteorological and electrical factors are consistently logged using a data acquisition device (Agilent 34970). Data, encompassing meteorological conditions (solar irradiance *(G)*, panel temperature *(T)*, and PV output *(I_{mpp}, V_{mpp}, P_{mpp})* metrics at the Maximum Power Point (MPP)), were gathered at intervals of 1 minute.

- The primary specifications of the chosen PV array utilized in this study are outlined in Table (3.1), with additional information about the entire PV setup available in [29].

Parameter	Description
Module technology	Mono-crystalline (mc-Si)
PV array nominal power	3.18 kWp
Inverter type and size	IG30 Fronius single-phase, 2.5 kW
Modules per inverter	30
Modules in series (Ns)	15
Strings in parallel (Np)	2
Tilt - Azimuth	35° - 10° West

Table (III.1): Main specifications of the selected PV array.

- Table (3.2) presents an overview of the essential electrical characteristics for the ISOFOTON 106-12 PV module at Standard Test Conditions (STC), which entail a temperature of 25°C and an irradiance level of 1000 W/m².

Parameter	Value
$P_{mp}(W)$	106
$I_{SC}(A)$	6.54
$V_{OC}(V)$	21.6
$I_{mp}(A)$	6.10
$V_{mp}(V)$	17.4
$\beta V_{OC}(\%/°C)$	-0.36
$\alpha I_{SC}(\%/°C)$	0.06

Table (III.2): Electrical characteristics of the considered PV module.

III.3 Suggestion approach for photovoltaic systems modelling

Our approach to photovoltaic (PV) modelling is founded on the commonly used one-diode model [30]. This model is widely embraced in PV module modeling across different technologies, including crystalline and thin-film configurations. Its popularity arises from its ability to balance model complexity with predictive precision. The solar cell's current-voltage *(I-V)* behavior is articulated by the implicit and nonlinear equation provided in Eq (III.1):

$$I = I_{ph} - I_o \left[exp\left(\frac{q(V+R_s I)}{nkT}\right) - 1 \right] \ldots\ldots\ldots\ldots\ldots\ldots \text{(III.1)}$$

Where I_o denotes the diode saturation current *(A)*, I_{ph}signifies the photocurrent *(A)*, and n represents the diode ideality factor. The Boltzmann constant ($1.38x10^{-23}JK^{-1}$) is denoted by *k*, while *T* represents the cell temperature in Kelvin *(K)*. The parameter *q* stands for the electrical charge ($1.602\ x10^{-19}C$), and *Vt(V)* denotes the thermal voltage, expressed as $V_t=k.T/q$. Finally, $R_{sh}$and $R_s$refer to shunt and series resistances *(Ω)*. For a comprehensive understanding of this model, including the necessary equations to extend its application from a single solar cell to an entire PV array, please refer to the detailed description provided in [31].

PV module manufacturers generally not directly supply the five parameters *Iph*, I_o, *n*, R_{sh}, and R_s. Research has shown that the actual values of these parameters, when extracted, frequently differ from those calculated using nominal data provided in the datasheet under Standard Test Conditions (STC) [32]. Therefore, achieving a precise correlation between the outputs of the PV model defined by Eq. (III.1) and real-world monitored data is crucial for accurate simulation and fault detection. Consequently, the importance of employing an effective parameter identification process cannot be overstated

III.4 Converting Current-Voltage Characteristics to Standard Conditions

In outdoor operating conditions, it is almost impossible to reach, at the same time, standard conditions (i.e., Gref = 1000 W/m^2, Tref = 25 °C). Therefore, an efficient mathematical analytical method that translates arbitrary I-V curves taken at any other temperature and irradiance than 1000 W/m^2 and 25 °C can be used to obtain reference curves [33]. The expressions given in Equations (III.2)and (III.3) are used to translate the short circuit current and the open-circuit voltage at their reference values *Isc,ref*and*Voc,ref*, respectively:

$$Isc,ref \quad (G_{ref}\ , T_{ref}) = I_{meas}(Gmeas\ , T_{meas})\frac{G_{ref}}{Gmeas} + \alpha\ (T_{ref}-, T_{meas}\ ) \ldots\ldots\ldots\ldots\ldots\ldots\ldots\ldots \text{(III.2)}$$

$$Voc,ref\ (G_{ref}\ , T_{ref}) = V_{meas}\ (Gmeas\ , T_{meas}) + n\frac{KB\,T}{q}\ln(\frac{G_{ref}}{Gmeas}) + \beta(T_{ref}-, T_{meas}\ ) \ldots\ldots\ldots\ldots \text{(III.3)}$$

- where α is the current temperature coefficient, β is the voltage temperature coefficient, their value is shown in Table 1, *n* is the modified ideality factor which is taken equal to the value given by the manufacturer, *Gmeas*and*Gref*are measured and reference irradiance in W/m2 respectively, *Tmeas*and *Tref*are measured and reference temperature in °C.

➢ The following mathematical expressions translate every point on the measured curve (*Vmeas*, *Imeas*) to the expected point on the translated reference curve (*Vref*, *Iref*):

$$I_{ref}=I_{meas}+\Delta Isc \ldots\ldots\ldots\ldots\ldots\ldots\ldots\ldots\ldots\ldots\ldots\ldots\ldots\ldots\ldots\ldots\ldots\ldots\ldots\ldots\ldots\ldots \text{(III.4)}$$

$$V_{ref}=V_{meas}+\Delta Voc \ldots\ldots\ldots\ldots\ldots\ldots\ldots\ldots\ldots\ldots\ldots\ldots\ldots\ldots\ldots\ldots\ldots\ldots\ldots\ldots\ldots\ldots \text{(III.5)}$$

where ΔIsc and ΔVoc are calculated by the following relations:

$$\Delta Isc = Isc,ref - Isc,meas \quad \text{(III.6)}$$

$$\Delta Voc = Voc,ref - Voc,meas \quad \text{(III.7)}$$

- For instance, figure (III,2) gives the translated curve from a measured I-V curve at (G_{meas}= 755 W/m2, T_{meas}= 27.2 °C).

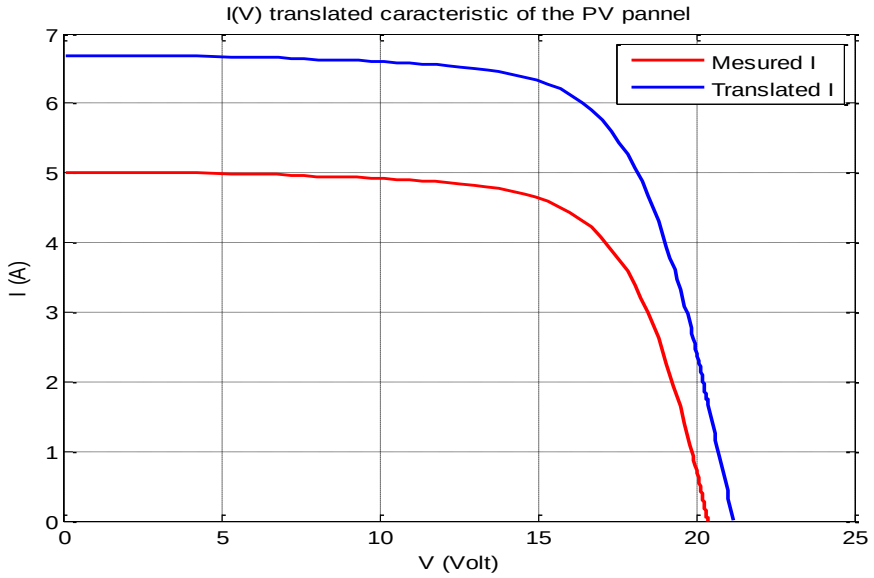

Figure (III.2): Measured and translated I-V curve to reference condition (G_{ref}= 1000W/m^2, T_{ref}=25°C) at (G_{meas} = 755 W/m^2, T_{meas} = 27.2 °C) for ISOFOTON 106 PV module.

III.5 Parameter Extraction using Moth Flam Optimization

In this section, we present a technique for offline parameter identification through optimization. We opt for this method due to the implicit nature of the characteristic equations in Eq. (1), posing challenges for direct parameter determination. Viewing the parameter identification process as an optimization problem, we employ the Moth Flam Optimization (MFO) algorithm to tackle this challenge. This algorithm effectively optimizes the unknown parameters to align with the implicit characteristic equations, enabling precise extraction of desired values based on actual measurement data. Our focus lies in quantifying the disparity between the outputs derived from Eq. (III.1) and the data obtained from the current-voltage translation method discussed earlier (section III.4). We employ the root mean square error (RMSE) as the primary metric for evaluating this difference (Figure (III.3)). For each set of experimental values *(I, V)*, the RMSE is calculated using the following formula:

$$RMSE = \sqrt{\frac{1}{N}\left(\sum_{i=1}^{N}\left(f(V,I,x)\right)^2\right)} \quad \text{(III.8)}$$

$$f(V,I,x) = I - \left(I_{ph} - I_o\left[exp\left(\frac{q(V+R_sI)}{nkT}\right) - 1\right] - \frac{V+R_sI}{R_{sh}}\right) \quad \text{(III.9)}$$

- In this context, x represents a vector comprising:

$$x = [I_{ph,ref}, I_{o,ref}, R_{sh,ref}, R_{s,ref}, n_{ref}]$$

while:

N =indicates the quantity of data points

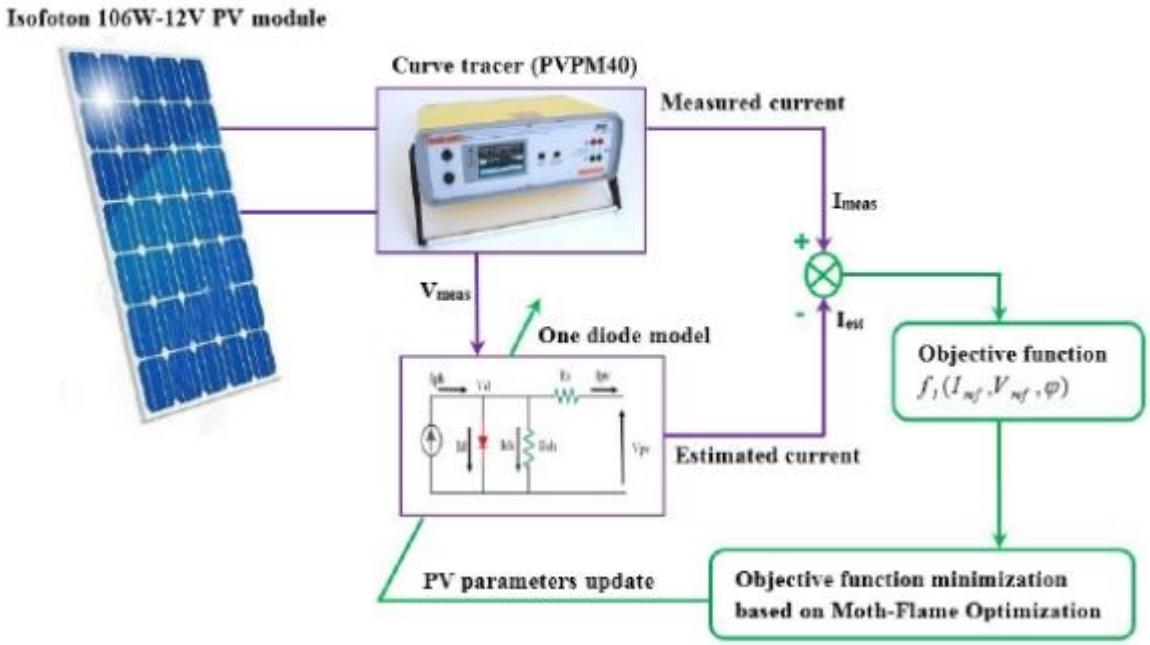

Figure (III.3): Flowchart for the identification of PV reference parameters based on Moth-Flame Optimization (MFO).

III.5.1 The Moth-Flame Optimization (MFO) algorithm

The Moth-Flame Optimization (MFO) algorithm is one of the optimizations and meta-heuristic algorithms that finds a way to solve problems by mimicking the behavior of moths near flames or fire. this algorithm was proposed in 2015 by Seyed Ali Mir Jalili [34]. the MFO algorithm, also known as the flame butterfly algorithm or simply the MFO algorithm, is a new exploratory model inspired by the nature and behavior of butterflies and their attraction to flames or fire.

The particularity of moths resides in the transverse orientation mechanism used to fly by night using the moon light waves. Moths maintain a fixed angle with moon allowing travelling in straight path for very long distances. Figure (III.4) presents a theoretical model of transverse orientation.

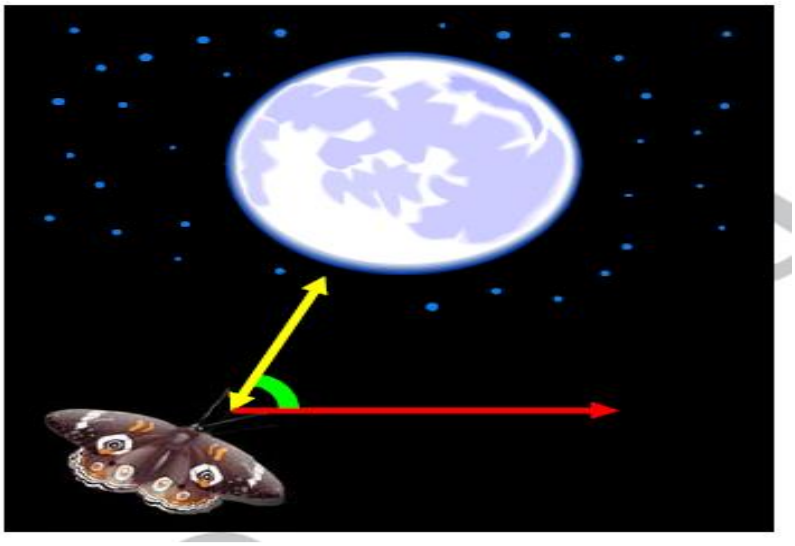

Figure (III.4): Transverse orientation

Assume the moon is on the south side of the sky and a person wishes to travel east. He could walk in a straight line toward the east if he kept the moon on his left side. Figure (III.5) shows the transverse orientation. Despite the effectiveness of transverse orientation, we typically see moths flying in a spiral around the lights. In fact, artificial lights fool moths, causing them to exhibit such behaviors. Figure (III.5) depicts a conceptual model of this behavior.

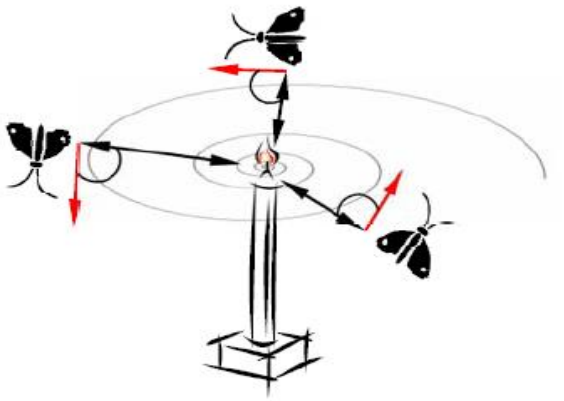

Figure **(III.5):**Spiral flying path around close light sources

The MFO algorithm assumes that the agents' solutions are moths and that the unkown variables are moth positions in space. As a result, the moths can fly in 1-D, 2-D, 3-D by varying their location vectors. Moths and flames are both solutions in the MFO algorithm which is a population-based approach [34]. The difference is the way that is treated and updated in each iteration. The moths represent actual search agents moving around the search space, whereas flames are the best position of moths that obtains so far. To clarify more, flames are considered as flags droppedby moths while searching the search space. Consequently, each moth searches around a flag and updates it when

better solutionis found. Based on this, a moth will never lose its best solution. Here, logarithmic spiral is defined for the MFO algorithm as follows:

$$S(M_i, F_i) = D_i e^{bt} \cos(2\pi t) + F_j \quad \text{(III.10)}$$

D_i can be computed as follows:

$$D_i = |F_j - M_i| \quad \text{(III.11)}$$

An adaptive mechanism to overcome the position updating is adopted for the number of flames.

$$Flame_{number} = round\left((N - l)\frac{N-1}{T}\right) \quad \text{(III.12)}$$

where *l*represents the actual number of iterations, *N*is theflames maximum number, and *T*indicates the maxiteration number. The detailed flowchartinFigure (III.6)illustrates the iterative process ofthe MFO algorithm.

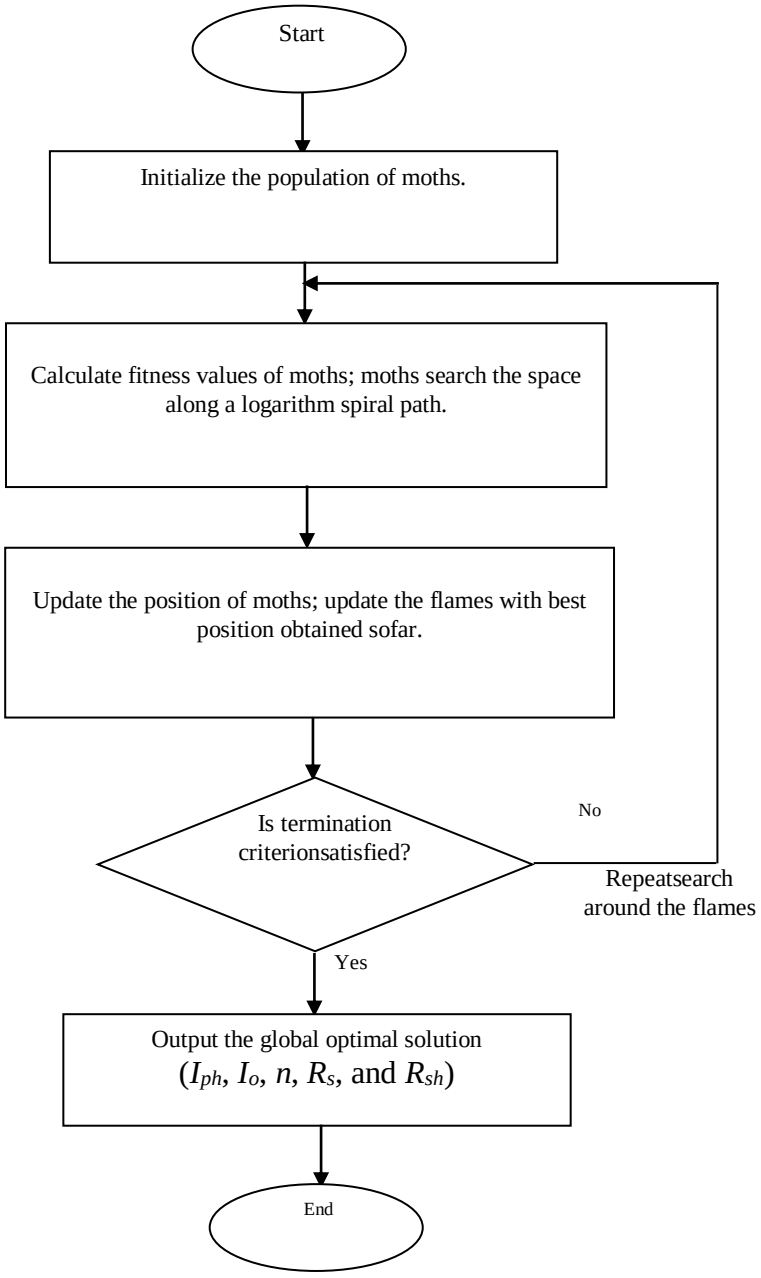

Figure (III.6): MFO algorithm flowchart.

III.6 prediction the photovoltaic (PV) outputs in real outdoor settings

The subsequent essential stage involves determining the values of the unknown parameters within real operating condition using fully analytical formulas and reference parameters derived from the MFO algorithm. Equations (III.13)to (III.18) sum up the analytical formulations that facilitate the computation of the five parameters in question as functions of temperature and irradiance [35–37].

$$n(T) = n_{ref}\left({}^{T}/_{T_{ref}}\right) \quad \text{(III.13)}$$

$$I_{ph}(G,T) = \frac{G}{G_{ref}}\left[I_{ph,ref} + \alpha\left(T - T_{ref}\right)\right] \quad \text{(III.14)}$$

$$R_{sh}(G) = R_{sh,ref}\left({}^{G_{ref}}/_{G}\right) \quad \text{(III.15)}$$

$$E_g = E_{g,ref}\left[1 - 0.0002677\left(T - T_{ref}\right)\right] \quad \text{(III.16)}$$

$$R_s(G,T) = R_{s,ref}\left(\frac{T}{T_{ref}}\right)\left[1 - \beta ln\left({}^{G}/_{G_{ref}}\right)\right] \quad \text{(III.17)}$$

$$I_o(G,T) = I_{o,ref}\left(\frac{T}{T_{ref}}\right)^3 e^{\left(\frac{q}{nK_B}\left(\frac{E_{g,ref}}{T_{ref}} - \frac{E_g}{T}\right)\right)} \quad \text{(III.18)}$$

- *Eg*represents the band gap energy of the semiconductor, while $E_{g,ref}$denotes the band gap energy under reference conditions. I_{ph}, I_o, n, R_s, and R_{sh}stand for the five parameters under actual operating conditions. Conversely, $Iph_{,ref}$, $I_{o,ref}$, n_{ref}, $R_{s,ref}$, and $R_{sh,ref}$refer to the five unknown parameters at the reference conditions determined through the application of the extraction algorithm.

Parameter	Value
R_p (Ω)	42.9633
R_S(Ω)	0.2212
I_o (A)	$4.344\ 10^{-7}$
n	45.1606
I_{ph}(A)	6.8378
RMSE	0.0122

Table (III.3): Extracted ODM parameters at STC.

- The proposed methodology for modeling the PV array has undergone extensive validation, employing the extracted parameters to simulate the PV array under varying irradiance (G) and

temperature (T) conditions, as described in equations (III13-III18). A comparison was made between the experimental I-V and P-V curves and the simulated data to evaluate the model's accuracy under static conditions. The results are depicted in figures III.7,III.8,III.9, and III.10, revealing a noteworthy agreement between the measurements and the simulated values. This observation is further corroborated by the RMSE indicator values, which stand at 0.0266 and 0.1024, respectively. Another study to confirm the accuracy of the parameter's extraction using MFO method is investigated. For this purpose, an experiment was conducted on the dynamic progression of MPP in a real working condition of grid connected PV system. To show this, the fitted model relied on the daily MPP progression was drawn versus real MPP report achieved for both semi-cloudy and cloudy sky Algerian situation. The actual PV array is composed of two strings connected in parallel; each one formed by fifteen ISOFOTON 106/12 PV modules connected in series. By means 1 minute as a sampling period, the data were recorded. Fig. (III.11), Fig (III.12) and Fig (III.13) present the time progression versus calculated power via the fitted model and real values respectively fora semi-clear, cloudy and cloudy sky condition.

From the simulation results, we notice an excellent fitting between the real and the calculated MPP values, which reveal the efficacy of the considered strategy.

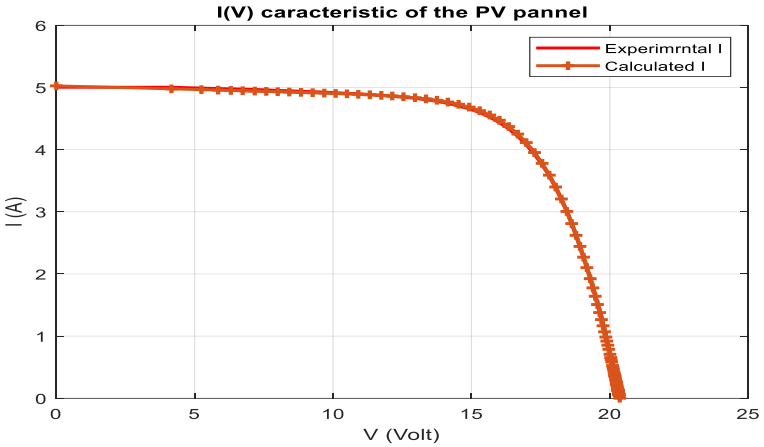

Figure (III.7): Measured and calculated IV curve of ISOFOTON106/12 PV module at T=28.1, G=749

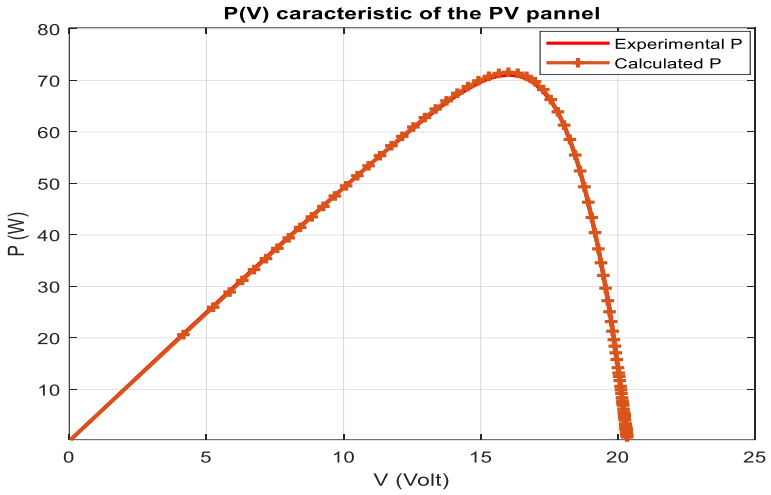

Figure (III.8): Measured and calculated PV curve of ISOFOTON106/12 PV module at T=28.1, G=749

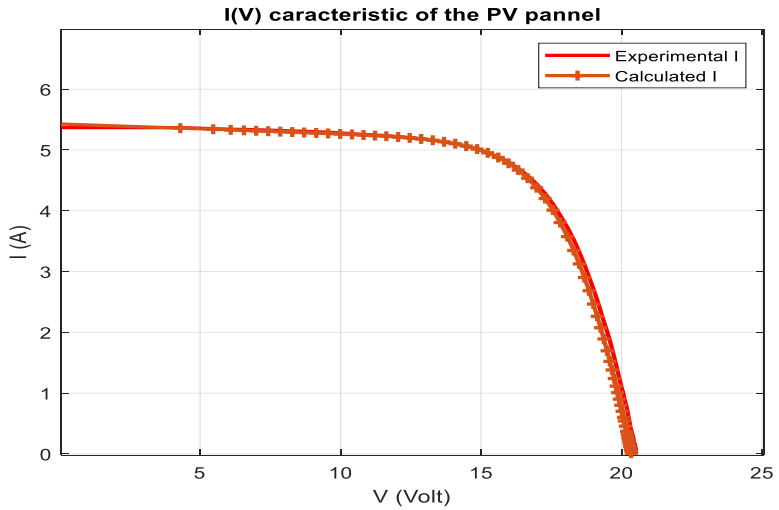

Figure (III.9): Measured and calculated IV curve of ISOFOTON106/12 PV module under T=28.2, G=800.

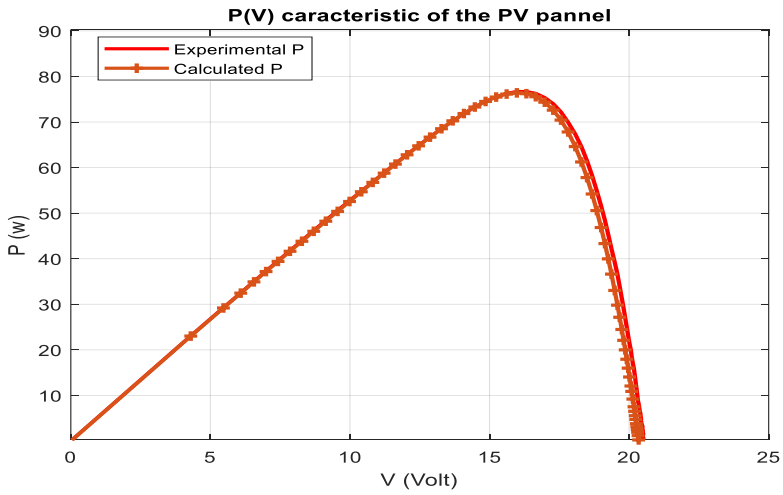

Figure (III.10): Measured and calculated PV curve of ISOFOTON106/12 PV module under T=28.2, G=800.

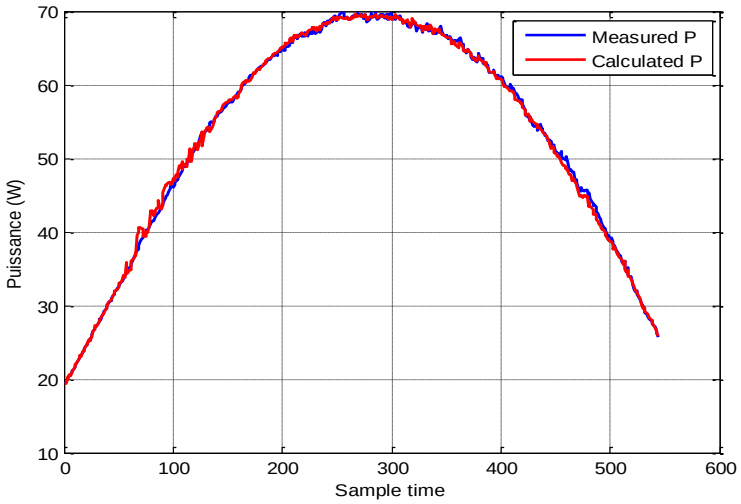

Figure (III.11): Comparison between measured and estimated P_{MPP} for a clear sky day.

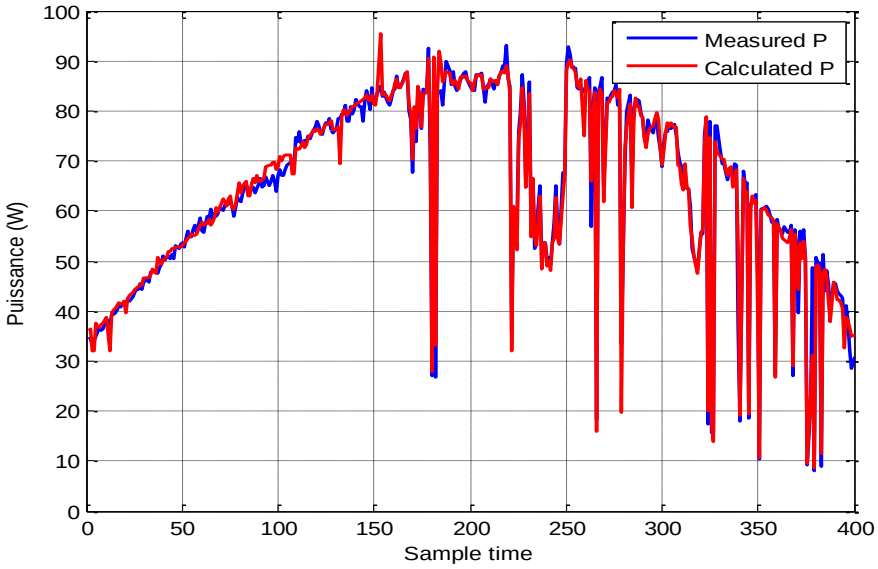

Figure (III.12): Comparison between measured and estimated P_{MPP} for a semi-cloudy day.

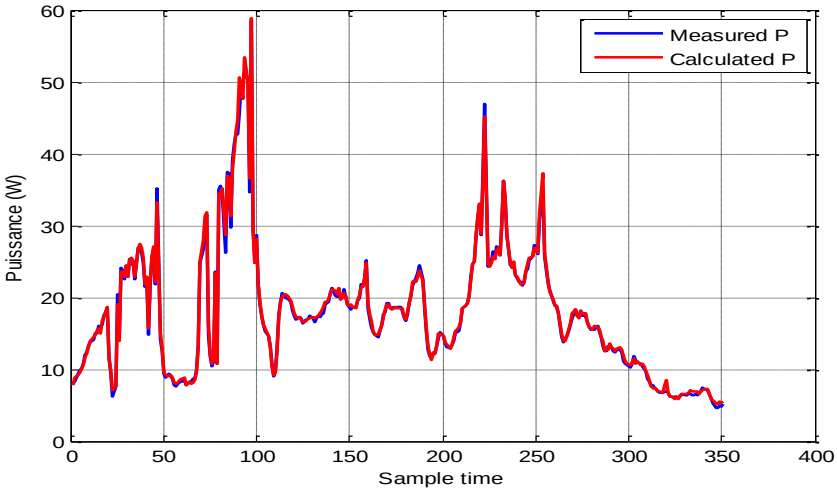

Figure (III.13): Comparison between measured and estimated P_{MPP} for a cloudy day.

III.7 Conclusion

In this chapter, an improved and precise method for extracting the five parameters of the single diode model of a PV module from the measured (I-V) curves is proposed. This methodology employs a hybrid approach combining both analytical and numerical methods, achieving extraction in three stages. First, the measured I-V characteristics under various irradiance and temperature conditions are translated into standard test conditions using analytical formulas, resulting in a unique I-V curve at reference conditions. Next, using the MFO algorithm as an optimization tool, the five parameters at these reference conditions are extracted. These parameters are then applied to the analytical expressions that describe PV modules under any operating conditions. The proposed approach's estimated results were validated against measured static data (I-V curves) and dynamic data (time evolution of *Impp, Vmpp,* and*Pmpp*). The results confirm the accuracy of this hybrid approach in properly estimating the five parameters, enabling the creation of an accurate model suitable for energy prediction and fault diagnosis purposes.

Conclusion and Perspective

Conclusion and Perspective

Solar photovoltaic energy comes from the direct conversion of a portion of solar radiation into electrical energy. This energy conversion is carried out by the photovoltaic cell, based on a physical phenomenon called the photovoltaic effect. The combination of several cells in series and/or parallel forms a photovoltaic generator, which has a nonlinear current-voltage characteristic presenting a maximum power point. Determining the parameters of this characteristic equation in real operating condition plays an important role in the precise modeling of solar cells.

After modeling and simulating the electrical operation of the cell as well as the photovoltaic generator under the influence of temperature, irradiance, the photocurrent, the diode saturation current, the diode ideality factor and series/parallel resistance, this work proposed a precise methodology for extracting the parameters of the PV module under real operating conditions. The suggested methodology combines numerical methods and analytical formulations of the single-diode model to derive the five unknown parameters under any operating conditions of irradiance and temperature. First, the (I-V) curves measured under random weather conditions are translated to standard test conditions (i.e., G = 1000 W/m², T = 25°C) using translation equations. The second step involves using the Moth flam optimization algorithm to identify the five parameters under standard conditions. Analytical formulations, at random irradiance and temperature, are then used to express the unknown parameters at any irradiance and temperature. The proposed approach will be validated under outdoor conditions against the measured I-V curves in various operating conditions. Dynamic validation is also performed where the measured values of the maximum power point (MPP) coordinates are compared to the actual dynamic MPP measurements of a grid-connected system located at the Renewable Energy Development Center (CDER) in Algiers

Based on the results obtained from the Matlab simulation, we can conclude that:

- Temperature and irradiance have a significant impact on the performance of the cells, and thus on the design and production of the PV generator.
- A good prediction model is directly based on the precise identification of the unknown parameters of the model, which govern the current-voltage relationship of the solar cell.

The main perspective of our work is to find and apply an effective machine learning techniques and supervised learning models to precisely estimate the power output from the considered Photovoltaic (PV) plants.

References:

[1] D. Sera, R. Teodorescu, and P. Rodriguez, "PV Panel Model Based on Datasheet Values", *IEEE International Symposium on Electronics*, ISIE 2007, Vigo, Spain, June 4-7, 2007.

[2] M. Chegaar, Z. Ouennough, F. Guechi, and H. Langueur, "Determination of Solar Cells Parameters Under Illuminated Conditions", *Journal of Electron Devices*, vol. 2, pp. 17 – 21, 2003.

[3] L. Han, N. Koide, Y. Chiba and T. Mitate,"Modeling of an Equivalent Circuit for Dye Sensitized Solar Cells", *Applied Physics Letters*, vol. 84, no.13, 2433.

[4] W. Xiao, MGJ Lind, W.G. Dunford and A. Capel,"Real-time Identification of Optimal Operating Points in Photovoltaic Power Systems". *IEEE Transactions on Industrial Electronics*, vol. 53, no.4, pp. 1017 – 1026, 2006.

[5] M. Ye, X. Wang and Y. Xu,"Parameter Extraction of Solar Cells Using Particle Swarm Optimization", *Journal of Applied Physics*, vol. 105, no. 9, 094502, 2009.

[6] T. Huld, R. Gottschalg and H.G. Beyer,"Topic M. Mapping the Performance of a PV modules, Effects of Module Type and Data Averaging", *Solar Energy*, no.84, pp. 324 -328, 2010.

[7] T. Easwarakhanthan, J. Bottin, I. Bouhouch and C. Boutrit,"Nonlinear Minimization Algorithm for Determining the Solar Cell Parameters with Microcomputers", *International* Journal *of Solar Energy*, vol. 4, no.1, pp. 1 – 12, 1986.

[8] A. Askarzadeh and A. Rezazadeh, "Extraction of maximum power point in solar cells using bird mating optimizer-based parameters identification approach," *Solar Energy*, vol. 90, pp. 123-133, 2013

[9] M.Ben Saad and A. Gnonlonfin, N. Khraief, M. Dimou"Les stratégies de développement des énergiesrenouvelables dans la région MENA :
Etude comparative et couloirs dedéveloppement ,"FEM43-04 FemiseResearchPapers, September2019.

[10] M. A,"Contributionà la commande MPPT pour les systèmes photovoltaïque ,"Thèse de Doctorat En vue de l'obtention du diplôme de Doctorat LMD, en Energies renouvelables en électrotechnique, University M'hamedBougara-Boumerdes, 2021/2022.

[11] https://www.connaissancedesenergies.org/lelectricite-dans-le-monde-en-2021-annee-de-records-220330.

[12] M. Ben Saad, A.Gnonlonfin, N.Khraief, and M.Dimou,"Lesstratégies dedéveloppement des énergies renouvelables dans la région mena : Etudecomparative et couloirs de développement. 2021.

[13]https://www.seia.org/initiatives/about-solar-energy.

[14]A.Bouraiou , A. Necaibia , N. Boutasseta , S. Mekhilef , R. Dabou , A. Ziane , N.Saho uane , I.Attoui , M.Mostefaoui , O.Touaba, " Status of renewable energy potential and utilization in Algeria "Journal of Cleaner Production",Vol. 246,27 December 2019.

[15] A.Ghaitaouiand, M.Hadji,"Extraction des Paramètres du Module Photovoltaïque installé dans un site saharien "Mémoire de Master en Physique Physique Énergétique et Energies Renouvelable,University Ahmed Draia -Adrar-,2021.

[16]A.Laghouag, **H.Bencheikh**,"Etude et simulation d'une cellule solaire àbase des éléments chalcogènes, Mémoire de Master Académique", Université Mohamed Boudiaf M'Sila, 2018/2019

[17]D.Hadjadj, O.Belkhiri,"Etude des Caractéristiques d'un Capteur Solaire Photovoltaïque et Evaluation de ses Performances sous Différentes Conditions Climatique" Mémoire de Master,University 08Mai 1945-Gulema, 2021/2022.

[18]A.Baadji, I.Chergui,"Extraction des Paramètres du Module photovoltaïque" 2018/2019.

[19]S.Sai and A.Kridlis,"Etude et simulation d'un système hybride (photovoltaïque/groupe électrogène)", Présenté en vue de l'obtention d'un diplôme de Master en Electromécanique, University Larbi Tebessi – Tébessa,2021/2022.

[20]S.Oufi,"Modélisation et commande d'un système de pompage photovoltaïque",Mémoire Magister, University Ferhat Abas- Setif-1 UFAS (Algerie), 2014.

[21]T.Bouguerra,"Optimisation d'un système photovoltaïque : Application en continu et en alternatif", Mémoire Magister, UniversityMentouri de Constantine1, 2014.

[22] M.Makhlouf,"Etude et optimisation d'un modèle de conversion d'énergie photovoltaïque application", thèse de doctorat, Université de Constantine, 2012.

[23]A.Saidani,"Amélioration de la technique d'extraction de maximum de puissance du système photovoltaïque basé sur la méthode (P&O) ", mémoire de master, Université de M'sila,2015.

[24] R. Arches,Y.**Cheron,B.Escaut,**"Convertisseurs continu-continu non isolés ",Institut Nationale Polytechnique de Toulouse.

[25] O. Gergaud, B. Multon, H. Ben Ahmed,"Analysis and Experimental Validation of Various Photovoltaic System Model",7th International ELECTRIMACS Congress, Montréal, Août 2002.

[26] M. Z. F.Z. Zerhouni,"Optimisation d'un système à énergie verte avec validation pratique," Revue des Energies Renouvelables, vol. 11, no. N°1, p. 41–49, 2008.

[27] A. Saadi, "Etude comparative entre les techniques d'optimisation des systèmes de pompage photovoltaïque," Université de Biskra Mémoire de Magister, 2000.

[28] A. Blorfan,"contribution à l'étude de l'association d'une source photovoltaïque et d'un filtre actif", thèse pour obtenir le grade de docteur de l'Université de Haute-Alasace.

[29] M. Zahra,"Modélisation de Modules Photovoltaïques" ,MémoiredeMagister en Microélectronique, Université de Batna,2012.

[30]I.hasni, A. El Mokeddem,"contribution à l'étude de l'association d'une source photovoltaïqueet d'un filtre actif", Mémoire de Master Université Djilali BounaamaKhemis Miliana, 2018.

[31] H. Belghitri et H. "Modélisation, simulation et optimisation d'un système hybride éolien-photovoltaïque", Mémoire de magister, 2009.

[32]N.Zehri,"Modélisation et Simulation d'un Système Photovoltaïque",Mémoire de Master en Automatique,Ecole Nationale Polytechnique, El Harrach,Juin 2015.

[33] A. Saadi, "Etude comparative entre les techniques d'optimisation des systèmes de pompage photovoltaïque," Mémoire de Magister, Université de Biskra, 2000.

[34] S. Mirjalili, "Moth-flame optimization algorithm: A novel nature-inspired heuristic paradigm", Knowl.-Based Syst., vol.89, pp.228–249, 2015.

[35] A. Chouder, S. Silvestre, N. Sadaoui, L. Rahmani, "Modeling and simulation of a grid connected PV system based on the evaluation of main PV module parameters". Simul. Model. Pract. Theory , vol.,20, pp. 46–58, 2012.

[36] A. Elkholy, A. El-Ela, "Optimal parameters estimation and modelling of photovoltaic modules using analytical method". Heliyon, 5, e02137, 2019.

[37] A.K.Tossa, Y.M. Soro, Azoumah, D. A. Yamegueu, "New approach to estimate the performance and energy productivity of photovoltaic modules in real operating conditions". Sol. Energy, vol. 110, pp. 543–560, 2014.